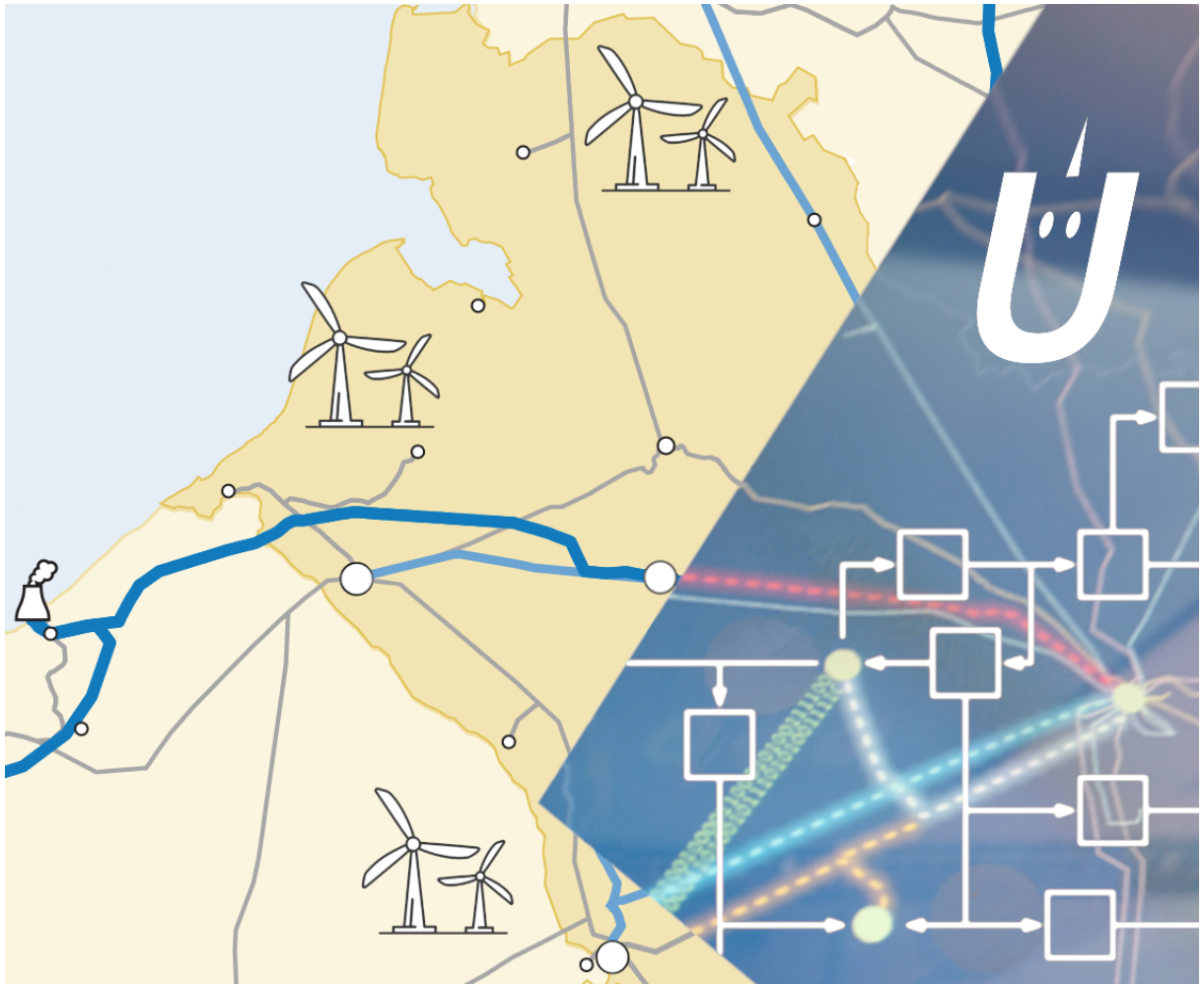




Final report dated 31.01.2022

# UNICORN

## A Unified Control Framework for Real-Time Power System Operation





# UNICORN

**Date:** 31.01.2022

**Location:** Bern

**Publisher:**

Swiss Federal Office of Energy SFOE  
Energy Research and Cleantech Section  
CH-3003 Bern  
[www.bfe.admin.ch](http://www.bfe.admin.ch)

**Co-financed by:**

ETH Zurich  
Automatic Control Laboratory  
Physikstrasse 3, 8092 Zürich  
[control.ee.ethz.ch](http://control.ee.ethz.ch)

RTE Réseau de transport d'électricité  
9 rue de la Porte de Buc, FR-78000 Versailles  
[www.rte-france.com](http://www.rte-france.com)

**Subsidy recipients:**

ETH Zurich  
Automatic Control Laboratory  
Physikstrasse 3, 8092 Zürich  
[control.ee.ethz.ch](http://control.ee.ethz.ch)

**Author:**

Saverio Bolognani, ETH Zurich, [bsaverio@ethz.ch](mailto:bsaverio@ethz.ch)  
Lukas Ortmann, ETH Zurich, [ortmannl@ethz.ch](mailto:ortmannl@ethz.ch)

**SFOE project coordinators:**

Dr. Michael Moser, [michael.moser@bfe.admin.ch](mailto:michael.moser@bfe.admin.ch)

**SFOE contract number:** SI/501708

**The authors bear the entire responsibility for the content of this report and for the conclusions drawn therefrom.**



## Summary

The project had the goal of engineering a control solution for power systems that enables and unifies multiple real-time control mechanisms (economic re-dispatch, line congestion control, voltage control), allowing the participation of active distribution networks as flexible providers of ancillary services. The proposed approach is based on a novel mathematical method for the design of feedback control laws that steer the power system state towards safe and efficient working points, ensure satisfaction of the grid operational constraints during the resulting transient, and guarantee the closed-loop stability of the grid dynamics. The resulting real-time strategy has the potential to outperform today's best practices and to ultimately enhance the system capacity to host intermittent renewable energy sources.

## Main findings

In this project, we successfully developed the necessary steps from a new control design methodology, *feedback optimization*, to its application to the real-time control of power systems. The project spanned multiple levels of technology readiness:

- New contributions to the mathematical foundation of feedback optimization have been derived, including closed loop stability certificates, robustness certificates, and proofs of stochastic convergence in the presence of noise.
- A control design procedure has been proposed, showing how the design of a feedback optimization controller can be performed by tapping into the literature of iterative nonlinear optimization and showing how input and output constraints can be incorporated.
- We identified scenarios of power system operations (both in transmission and distribution networks) where feedback optimization can replace today's real-time control mechanisms and ancillary services.
- For these scenarios, we produced public numerical benchmarks and we set up simulation environments that allow to assess the performance of the proposed controllers.
- We verified that the proposed control strategy, when applied to these scenarios, outperforms the current state of the art (grid codes and industrial standards, both in distribution grids and subtransmission grids).
- We delivered a proof-of-concept prototype that successfully demonstrated, in a real experiment, that the proposed control strategy can be used for the real-time control of a power system.

In conclusion, the project demonstrated that feedback optimization can be used to design automated controllers for the real-time operation of the grid, and more specifically for reactive power compensation, active power curtailment, voltage regulation, tap changer control, losses minimization, line congestion control, and economic redispatch. While, as anticipated, these different tasks and functions can coexist in the same unified controller, we have identified some particularly promising setups, e.g., voltage regulation via reactive power compensation and tap changer control. Future steps include the engineering of these solutions for a real application to a power grid, the use of similar controller strategies for emergency operations after contingencies, and the possibility of a *virtual reinforcement* of transmission and distribution grids via dispersed intelligence and feedback control instead of new infrastructure.



## Contents

<b>1</b>	<b>Introduction</b>	<b>5</b>
1.1	Background information and current situation	5
1.2	Purpose of the project	5
1.3	Objectives	6
<b>2</b>	<b>Procedures and methodology</b>	<b>6</b>
2.1	WP1 Mathematical foundation of feedback optimization	6
2.2	WP2 Real-time power system operation	7
2.3	WP3 Engineering and experimental validation	8
<b>3</b>	<b>Results and discussion</b>	<b>9</b>
3.1	WP1 Mathematical foundation of feedback optimization	9
3.2	WP2 Real-time power system operation	18
3.3	WP3 Engineering and experimental validation	36
<b>4</b>	<b>Conclusions and next steps</b>	<b>40</b>
<b>5</b>	<b>International cooperation</b>	<b>41</b>
<b>6</b>	<b>Communication and dissemination</b>	<b>41</b>
6.1	Public website and benchmarks	41
6.2	Talks, tutorial, presentations	41
<b>7</b>	<b>Publications</b>	<b>43</b>
	<b>References</b>	<b>44</b>



# 1 Introduction

## 1.1 Background information and current situation

Today's power system operation is structured into multiple time scales. The objective of the transmission system operator in the day-ahead stage is to identify the most economical generation dispatch (possibly via an energy market) that, according to a grid model, satisfies the operational constraints of the power system (line limits, generator limits, reliability requirements, etc.). In real-time, this schedule needs to be "converted" into set-points for the low-level controllers that actuate the grid, for example, generation and voltage set points for the synchronous generators. These set-points can deviate from the original schedule if unanticipated contingencies (e.g. increased or decreased generation and load, line faults, generator downtime) require so. Today, this is done mostly in an operator mediated way, via a number of procedures that restore system frequency, inter-area power flows, voltage profiles, and line currents. These sporadic emergency procedures are mostly based on operator expertise and on extensive simulation studies.

This approach won't suffice in future power systems. In fact, the integration of significant amount of fluctuating renewable power generation will introduce frequent voltage contingencies and congestion in the grid. As this generation is dispersed across the grid, an exhaustive simulation study of the possible contingencies is doomed to be impractical. On the positive side, future power grids will feature ubiquitous real-time data and better communication technologies that will make state estimation and data fusion more reliable, affordable, and practical. Moreover, actuation capabilities in future power grids will include not only synchronous generators but also a number of controllable devices (microgenerators, compensators, dispatchable loads, transformer tap changers) connected to the subtransmission and the distribution layer and capable of providing these ancillary services as a finely distributed network of actuators.

Driven by these challenges and opportunities, there is a recent interest in the idea of controlling a power system in real-time, in feedback interaction with the grid, so that the closed-loop system converges to (and tracks) the solution of an optimal power flow problem. Although some of the key ideas on feedback regulation of the set-points of a power system have been explored before towards specific objectives (e.g. optimal frequency control, voltage regulation, wide-area balancing – see section IV in the survey paper [1]), attempts to generalize these to generic AC OPF problems are not more than a few years old [2] [3] [4] [5]. These works tackle this challenging problem with the tools of iterative optimization and nonlinear programming, and rely on the assumption that the set-points are instantaneously tracked by the power system dynamics, which include both the physics of the grid and the transients of the local low-level controllers. Critical unresolved aspects of this approach are how to handle operational constraints, how to guarantee satisfactory behaviors in the case of model mismatch, and how to certify the stability of the resulting closed-loop dynamic behavior of the grid (controller dynamics + grid dynamics). This project tackles these questions by building on a novel geometric model of power system steady state solutions [6] and on the mathematical abstraction of the dynamic problem as a projected gradient flow on manifolds [7]. This approach allows to design the closed-loop behavior of these control strategies in the presence of constraints on the real-time trajectory of the system and in for complex grid models that include multiple classes of distributed energy resources.

## 1.2 Purpose of the project

This project proposes a replacement for today's real-time operation procedures with a persistent unified control approach capable of reliably steering the power system state along trajectories that

1. satisfy operational constraints of the grid (e.g. line limits, voltage limits) at all times
2. maintain grid dynamical instability in closed-loop
3. are economical (i.e., minimize the deviation from the original schedule).



Ultimately, the proposed real-time control strategy

- makes the grid more resilient against unanticipated contingencies
- allows larger penetration of fluctuating renewable energy sources
- enables the participation of active distribution networks to the provision of ancillary services.

### 1.3 Objectives

The project delivered the following three outcomes.

- A novel methodology for real-time power system operation design
  - A set of mathematical methods that advance the state of the art in feedback optimization.
  - Rigorous analytical guarantees of stability and performance of complex dynamical systems whose steady state is controlled in closed-loop according to the proposed paradigm.
  - Numerical certificates of stability for the closed-loop behavior that can be verified on the model of a power system controlled via the proposed unified control scheme.
- A new control architecture for real-time power system operation
  - A detailed description of how the proposed control strategy can be integrated in today's grid operations, what ancillary services it can replace, and how it would practically interface with day-ahead scheduling on one hand and local controllers on the other hand.
  - Numerical method for practical design and tuning of the unified control scheme and for the evaluation of its robustness to model mismatch and measurement noise.
  - A series of relevant scenarios in which the proposed approach outperforms traditional partially-automated grid operation strategies in terms of grid resilience, security, and performance.
- A proof-of-concept prototype
  - A demonstration of how, based on technological but also regulatory considerations, the features of the solution derived in this project can be deployed on a real power system.
  - An example of the performance gain that can be achieved by adopting the proposed control scheme as a replacement for today's industrial practice.

## 2 Procedures and methodology

The project is structured into three separate Work Packages.

### 2.1 WP1 Mathematical foundation of feedback optimization

The novelty of the proposed approach requires the derivation of original mathematical results, along the following lines.

#### D1.1 Projected dynamical systems for real-time optimization

The problem of real-time control of a power system is mathematically abstracted as a problem of optimization on manifolds, using the geometric model that constitute the basis of the proposed control design approach. We explored different methods to construct system trajectories that



1. belong to the manifold at all times
2. satisfy operational constraints
3. converge to the solution of a cost-minimization problem.

To do so, we adopted the formalism of projected dynamical systems, extending and generalizing the results available in the literature in order to apply them to dynamics on manifolds. We derived conditions for the mathematical well-posedness of the problem.

For the design of the optimizing feedback controller, we tapped into the literature of nonlinear optimization and experiment with both projected gradient descent algorithms and saddle flows. For these methods, we derived local convergence guarantees for the resulting non-convex optimization problem.

### **D1.2 Certificates of stability for feedback optimization**

In order to derive certificates of stability of the closed loop system (which includes both the dynamic behavior induced by the real-time optimization algorithms – on the manifold – and the dynamics of the low level controllers – transversally to the manifold) we analyzed the resulting multi-time-scale system via the tools of singular perturbation analysis. We derived certificates of stability, i.e. analytical or numerical tests that guarantee attractiveness of the manifold and can exclude any detrimental interaction between the system dynamics and the real-time optimization algorithms.

## **2.2 WP2 Real-time power system operation**

In this second workpackage, the results derived in WP 1 have been applied in order to derive a control solution for real-time operation of power systems.

### **D2.1 Power system operation scenarios**

In order to assess the practical relevance of the proposed approach for power system operation, some realistic scenarios have been identified. These scenarios could include both persistent regulation problems and contingencies (e.g. redispatch following a drop in power generation). Two kind of scenarios have been sought for:

- specialized scenarios that involve one or few ancillary services, in order to provide the benchmark for a comparison of the proposed approach with today's state of the art
- complicated multi-objective scenarios, in order to motivate this novel unified approach and illustrate its potential to tackle high-complexity problems that are currently unexplored. Moreover, some deliberately small-scale yet insightful scenarios have been included in order to illustrate challenging cases in which the main features of the proposed solution (and in particular the any-time satisfaction of the operational constraints) can be verified.

### **D2.2 Real-time power system operation**

Relevant ancillary services (e.g. frequency regulation, voltage regulation, reactive power compensation, line congestion control) have been formulated as a unified optimization problem like prescribed by the results of WP1, and therefore encoded in

- a cost function (the control effort, to be minimized)
- decision variables (the set-points that can be commanded)



- soft constraints (penalties on violations)
- hard constraints (strict operating limits).

All these problem parameters are possibly time-varying, because of fluctuating inflow of renewable generation, environment-dependent line limits, variations in load, etc. The proposed real-time controller has been validated in simulations, in order to

- verify the effectiveness of the approach on the scenarios identified before
- check stability of the closed loop system as predicted by the theoretical results
- assess the transient tracking performance of the proposed solution.

Numerical simulations incorporated real data provided by RTE, in order to co-simulate generation fluctuation and regulation mechanisms.

## **2.3 WP3 Engineering and experimental validation**

In this last Work Package, the practicality of the proposed approach will be analyzed, how it could be integrated in today grid's operation, and how the unified control scheme should be engineered.

### **D3.1 Control robustification**

The proposed feedback approach was expected to outperform model-based optimal dispatch when the systems is affected by noise in the measurements and uncertainty in the model parameters and model mismatch. With respect to the noisy input data, as the proposed control approach require real-time acquisition of the state of the system, a state estimation procedure will have to be integrated into the feedback loop. Three questions have been addressed:

- whether the data processing delay introduced by the state estimation procedure has any detrimental effect on the dynamics of the closed loop system;
- whether state estimation can enable the application of the proposed approach to practical scenarios in which full state measurement is not available, and what is the effect on the tracking performance;
- whether it is possible to distribute the problem in a multi-agent architecture in order to enhance scalability and modular deployment.

On the other hand, the robustness of the proposed feedback approach to model uncertainty has been verified both extensive numerical experiments and proof-of-concept implementations on real testbeds.

### **D3.2 Proof-of-concept prototype**

As the proposed real-time control solution aims at being embedded in today's power system operations, the interface of the proposed feedback scheme with existing dispatch protocols (for actuation) will be examined. This will be done via a proof-of-concept demonstration on an experimental distribution feeder, with a specific focus on the problem of voltage regulation and reactive power compensation via controllable power converters.

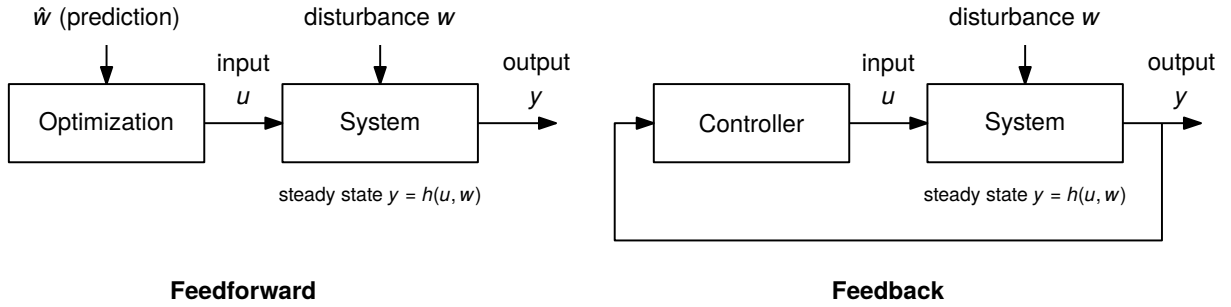


**Figure 1:** A schematic illustration of the difference between the standard optimization approach and the proposed feedback solution.

### 3 Results and discussion

We hereafter present the main results of each Work Package, organized according to the same structure as in Section 2. Throughout this section, we refer to the relevant open-access project publications where further details can be found.

#### 3.1 WP1 Mathematical foundation of feedback optimization

##### D1.1 Projected dynamical systems for real-time optimization

The key theoretical idea behind the methods proposed in this project consists in interpreting iterative optimization algorithms as robust controllers, and interconnecting them to the plant that we want to steer to efficient operations, instead of employing them to compute this optimal configuration offline and then command it to the plant (see comparison in Figure 1). This idea is developed and illustrated in detail in the review paper [8], where we also contrast it to other approaches like model predictive control, extremum seeking, modifier adaptation, real-time iteration, and others.

Here, we present a simple yet insightful example of this concept, namely a gradient system interconnected with a physical plant.

Consider a dynamic nonlinear plant

$$\dot{\zeta} = f(\zeta, u) \quad y = g(\zeta) + d, \quad (1)$$

where  $\zeta$ ,  $u$  and  $y$  are the state, input, and output, and  $d$  denotes an additive disturbance. The vector field  $f(\cdot, \cdot)$  and the map  $g(\cdot)$  describe the process and output measurement, respectively.

We assume that, for any fixed  $u$ , the plant is asymptotically stable with fast-decaying transients such that, for every  $u$ , there exists a unique steady state  $\hat{h}(u)$  such that  $0 = f(\hat{h}(u), u)$ . Consequently, there also exists a *steady-state map*  $h(u) := g(\hat{h}(u))$ . We assume  $h$  to be continuously differentiable in  $u$ .

We wish to minimize a cost  $\Phi(y)$  which is a function of the plant output  $y$ . Given  $h$  and  $d$ , we may equivalently minimize the *reduced* cost  $\tilde{\Phi}(u) := \Phi(h(u) + d)$  instead. For this purpose, we consider a simple gradient flow

$$\dot{u} = -\nabla \tilde{\Phi}(u)^T = -\nabla h(u)^T \nabla \Phi(h(u) + d)^T, \quad (2)$$

where  $\nabla h(u)$  is due to the chain rule applied to  $\Phi(h(u) + d)$ .

The gradient flow (2) is a closed system. However, recognizing  $h(u) + d$  as the measurable output  $y$ , (2) can be easily transformed into an open system and interconnected with the plant (1) as shown in Figure

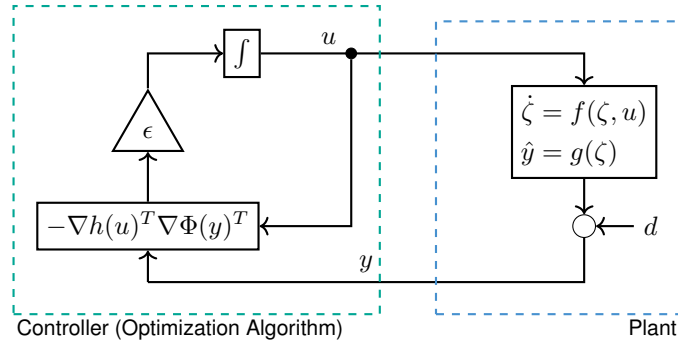


**Figure 2:** Simple feedback-based gradient flow

2. This yields the closed-loop dynamics

$$\begin{aligned} \text{plant} \begin{cases} \dot{\zeta} &= f(\zeta, u) \\ y &= g(\zeta) + d \end{cases} \\ \text{controller} \begin{cases} \dot{u} &= -\epsilon \nabla h(u)^T \nabla \Phi(y)^T, \end{cases} \end{aligned} \quad (3)$$

where  $\epsilon > 0$  is a scalar control gain.

The systems (1), (2) and (3) can be understood from a *singular perturbation* viewpoint [9, Chap. 11]: As  $\epsilon \rightarrow 0^+$ , the plant behavior is replaced by the algebraic map  $h$ , and the remaining dynamics (2) are the “slow” *reduced system*. Conversely, on a fast timescale, on which  $u$  and  $d$  can be assumed to be constant, the plant dynamics (1) are referred to as the “fast” *boundary-layer system*.

Thanks to the integral control structure of (3), it can be easily seen that any equilibrium point  $(\zeta^*, u^*)$  of (3) is a steady-state of the plant and satisfies  $\nabla \tilde{\Phi}(u^*)^T = \nabla h(u^*)^T \nabla \tilde{\Phi}(h(u^*) + d)^T = 0$ . Therefore,  $u^*$  is a critical point of  $\tilde{\Phi}$  (and a minimizer if  $\tilde{\Phi}$  is convex).

Crucially, the controller in (3) does not require explicit knowledge of  $h$  (nor of  $f, g$ ). Instead, only the cost function gradient  $\nabla \Phi(y)$  as well as steady-state input-output sensitivities  $\nabla h(u)$  are required. Moreover, the additive disturbance  $d$  does not need to be known or explicitly estimated and is fully rejected, i.e., an equilibrium is a critical point of  $\Phi(h(u) + d)$ , independently of the value of  $d$ .

This simple example illustrates the key idea that guided the design of feedback optimization controllers in the rest of the project. In fact, by tapping into the literature of iterative algorithms for nonlinear optimization, a designer can extend this approach to more complicated setups, for example by incorporating constraints on the plant inputs and outputs.

In what follows, let us consider the concatenated system state  $x := \begin{bmatrix} u \\ y \end{bmatrix}$ , and we allow cost functions  $\Phi(x)$  (an extension of the small example that we just presented).

A relatively easy and widely applicable way to incorporate them into an optimization problem are the addition of penalty (or regularizing) or barrier terms to the objective. For a constraint of the form  $c(x) \leq 0$  where  $c : \mathbb{R}^n \rightarrow \mathbb{R}$  is continuously differentiable, a common penalty function is for example the squared 2-norm of the constraint violation vector, i.e.,  $\phi(x) = \frac{\rho}{2} \|\max\{c(x), 0\}\|^2$  where  $\rho > 0$  denotes a scaling parameter. Many variations, including different norms on constraint violations are possible. The common feature of penalty function lies in the fact that they technically allow for constraint violations, i.e., minimizers of a penalty-augmented cost function  $\Phi(x) + \phi(x)$  do not generally satisfy  $c(x) \leq 0$ . A notable exception are so-called *exact penalty methods* that transform a constrained optimization problem into an unconstrained one without changing the location of minimizers, albeit at the expense of smoothness or other technical drawbacks.

Barrier functions, on the other hand, can be used to apply constraints strictly, i.e., without allowing for any violation. For this purpose, a barrier function  $\psi(\cdot)$  for the constraint  $c(x) \leq 0$  needs to be such that for  $x \rightarrow x^*$  with  $c(x^*) = 0$  we have  $\psi(x) \rightarrow \infty$ . A common example satisfying this condition are



negative log-barriers of the form  $\psi(x) = -\frac{1}{\mu} \log(c(x))$  which are important for interior-point methods for constrained convex programming.

To enforce unilateral (i.e., inequality) constraints it is often possible to rely on projection mechanisms. In a computational context, this is particularly true if the projection onto a given constraint set is easy to evaluate numerically.

Consider the constrained optimization problem

$$\text{minimize } \Phi(x) \quad \text{subject to } x \in \mathcal{X}, \quad (4)$$

where  $\mathcal{X} \subset \mathbb{R}^n$  is closed convex and non-empty, and  $\Phi$  is continuously differentiable. The classical *projected gradient descent* to solve this problem takes the form

$$x^{k+1} = P_{\mathcal{X}}(x^k - \alpha^k \nabla \Phi(x^k)^T). \quad (5)$$

where  $P_{\mathcal{X}}(y) := \arg \min_{x \in \mathcal{X}} \|x - y\|$  denotes the Euclidean minimum norm projection onto  $\mathcal{X}$ , and  $\{\alpha^k\}$  is a sequence of step sizes. By choosing infinitesimally small step-sizes, the continuous-time limit of (5) is a *projected gradient flow*. The qualitative behavior of projected gradient flows is as follows: in the interior of the feasible set, trajectories follow the gradient direction whereas at the boundary, trajectories follow the steepest *feasible* descent direction. Compared to penalty or barrier approaches, projected gradient flows are inherently discontinuous systems, and their study requires tools from non-smooth analysis. Projected gradient flows extend properties from their unconstrained counterparts. For instance, similarly to standard gradient flows, trajectories of (5) converge to the set of critical points (in this case, Karush-Kuhn-Tucker points of (4)).

Finally, constraints can be enforced by employing saddle-point flows. Consider the problem

$$\begin{aligned} &\text{minimize } \Phi(x) \\ &\text{subject to } x \in \mathcal{X} \\ & \quad \quad \quad g(x) \leq 0, \end{aligned} \quad (6)$$

where  $\Phi$  and  $g$  are convex (but not necessarily strictly convex) and continuously differentiable. Further, let  $\mathcal{X} \subset \mathbb{R}^n$  be non-empty and closed convex. We may define the *partial* Lagrangian  $L : \mathcal{X} \times \mathbb{R}_{\geq 0}^m \rightarrow \mathbb{R}$  of (6) as

$$L(x, \mu) := \Phi(x) + \mu^T g(x), \quad (7)$$

and note that  $\mu$  must lie in the non-negative orthant  $\mathbb{R}_{\geq 0}^m$  because it is associated with an inequality constraint.

To find a saddle-point of  $L$  on the set  $\mathcal{X} \times \mathbb{R}_{\geq 0}^m$ , we consider the *projected saddle-point flow*

$$\dot{x} = \Pi_{\mathcal{X}} \left[ \underbrace{-\nabla \Phi(x)^T - \nabla g(x)^T \mu}_{-\nabla_x L(x, \mu)^T} \right] (x) \quad (8)$$

$$\dot{\mu} = \Pi_{\mathbb{R}_{\geq 0}^m} \left[ \underbrace{\nabla_{\mu} L(x, \mu)^T}_{g(x)} \right] (\mu) \quad (9)$$

where  $\Pi_{\mathcal{X}}[w](x)$  and  $\Pi_{\mathbb{R}_{\geq 0}^m}[v](\mu)$  project  $w$  and  $v$  onto the tangent cone of  $\mathcal{X}$  and on the non-negative orthant  $\mathbb{R}_{\geq 0}^m$  at  $x$  and  $\mu$ , respectively. Consequently, trajectories of (8) cannot leave  $\mathcal{X} \times \mathbb{R}_{\geq 0}^m$ .

Importantly, two different constraint enforcement mechanisms are at play in (8). On one hand, the constraint  $x \in \mathcal{X}$  is enforced directly by projection. The constraint  $g(x) \leq 0$  on the other hand is enforced by dualization. Namely, the dual variable  $\mu$  is updated in response to a constraint violation  $g(x) > 0$  and converges to a dual solution of (6).

Under weak technical assumptions and if  $\Phi$  is strictly convex, trajectories of (8) are guaranteed to converge to a Karush-Kuhn-Tucker point (and thereby to a global optimizer) of (6). However, convergence

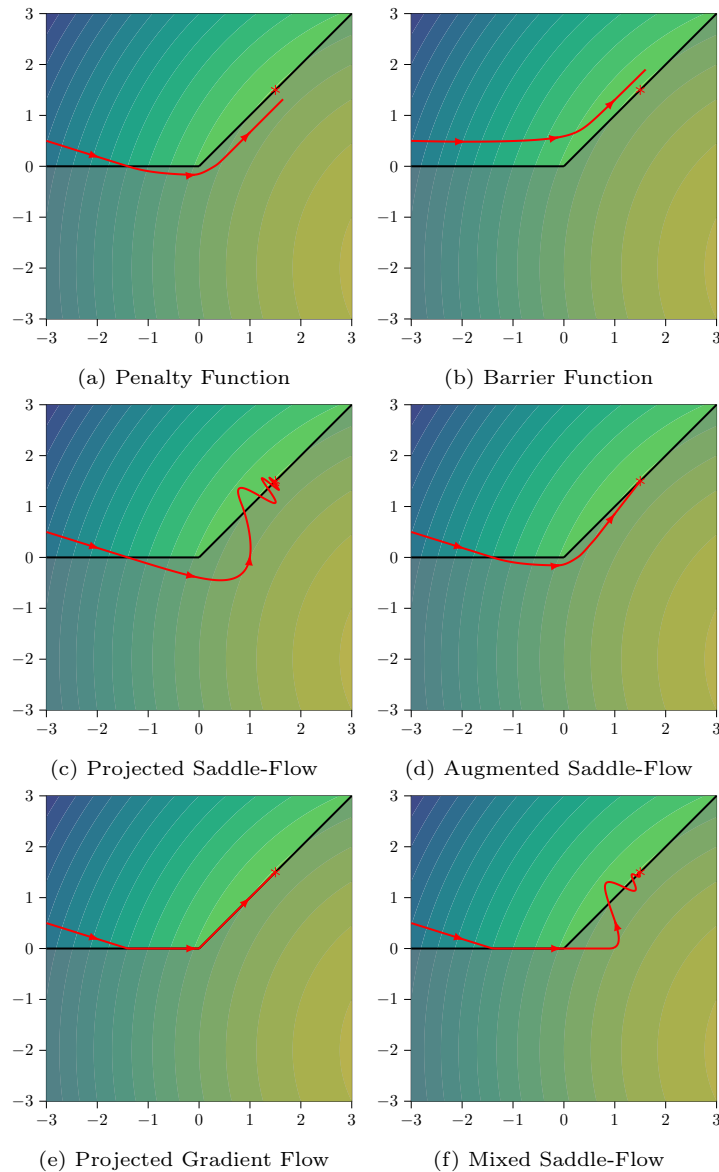


**Figure 3:** Behavior of different constraint enforcement mechanisms

All panels show the minimization of a quadratic function subject to two constraints  $x_2 \geq 0$  and  $x_2 \geq x_1$  (the grayed out area is infeasible). Penalty (a) and barrier (b) functions allow for smooth outer and inner approximations of constraints with an unconstrained gradient flow. Saddle-point flows (c) enforce constraints only asymptotically by integrating constraint violation over time, but are often amenable to a distributed implementation. Augmenting saddle-point flows with a penalty term can improve convergence (d). Projected gradient flows (e) enforce constraints directly by projection, which results in non-smooth trajectories, but their implementation is not immediate. Individual constraints can also be enforced with a combination of these mechanisms, e.g., as in (f) with a projection for  $x_2 \geq 0$  and dualization (saddle-point flow) for  $x_2 \geq x_1$ .

and stability results for non-convex problems are not generally available. Moreover, even for convex problems, tuning can be difficult, especially for nonlinear problems. Suboptimal parameter choices can lead to severely under- or over-damped transients that may venture far outside the feasible domain, which is undesirable in online and closed-loop applications. This problem gets only more challenging for high-dimensional and ill-conditioned problems.

We have presented several ways to design dynamics that can solve constrained optimization problems. Their characteristic behaviors and different combinations are illustrated in Figure 3. In the following, we



summarize, contrast, and compare these different mechanisms.

Penalty and barrier functions can be used to transform problems into unconstrained problems which can then be tackled with a simple gradient flow. However, both approaches by themselves can enforce constraints only approximately. Barrier functions achieve an “inner” (i.e., conservative) approximation, whereas penalty functions generally allow for a small constraint violation and thus constitute an “outer” approximation. Both approaches are widely applicable (under minor technical assumptions) and do not require convexity of the constraints. However, theoretical guarantees often rely on additional assumptions and, because of practical considerations, penalty and barrier function cannot be chosen arbitrarily steep.

Constraint enforcement by (infinitesimal) projection, as for continuous-time projected gradient flows, is mathematically well-posed and works in very general settings. In particular, convexity of the constraint set is not generally required (as opposed to discrete-time projected gradient descent). Furthermore, constraints are represented exactly and satisfied at all times. However, these continuous-time discontinuous dynamical systems are often not directly implementable. Instead, discrete-time approximations, for example, rely upon the fact that the numerical projection onto the feasible constraint set are computationally inexpensive. In continuous-time, projected dynamical systems can be implemented by exploiting physical saturation and applying anti-windup control. Another possibility, to approximate projected gradient flows, is by appropriate discretization which, in contrast to (5), do not require an explicit projection  $P_{\mathcal{X}}$  onto the feasible set.

Dualization of constraints leads to saddle-point flows where dual variables are computed by integrating the constraint violation over time. Hence, transient constraint violation are generally unavoidable. For an inequality constraint, the corresponding dual variable must be kept non-negative by projection. Formal convergence guarantees are available only for convex problems (or with dual augmentation which alters equilibrium points) and, in practice, this method is difficult to tune, but often allows for distributed implementation that requires only the communication of dual multipliers.

In theory, each constraint (in functional form) can be enforced with one these mechanisms independently of the other constraints. For example, in panel (f) of Figure 3, the constraint  $x_2 \geq 0$  is enforced by projection whereas  $x_2 \geq x_1$  is dualized. This freedom of choice is particularly useful in control setups where the real-world nature of constraints can dictate the appropriate enforcement mechanism. For instance, barrier functions may be considered for constraints that may not be violated under any circumstances. Constraints that are naturally enforced by physical saturation, mechanical constraints or similar are best represented by projections. Dualization in combination with a penalty term is particularly helpful to enforce constraints asymptotically and often allow for distributed implementations.

All of these constraint enforcement methods can be applied in an online feedback setup, albeit their suitability depends on the specific constraint type, problem size and available model information.

## D1.2 Certificates of stability for feedback optimization

One of the challenges that arise when an optimization flow (e.g., a gradient flow) is interconnected to a physical plant is *closed-loop stability*. The idea that plant dynamics in (3) need to be fast-decaying is indeed crucial as the following numerical example shows.

Consider the objective  $\Phi(y) = (y^2 - 1)^2$  which is illustrated in the top left panel of Figure 4 and has two isolated minima  $\{-1, 1\}$ . Consider a single-input-single-output second-order plant governed by

$$\ddot{\zeta} + a\dot{\zeta} + b(\zeta - u) = 0$$

with  $a = 2$  and  $b = 25$  and  $y = \zeta$ . The plant is asymptotically stable, under-damped, and, at steady state, we have  $y = \zeta = u$ . Hence, the controller in (3) takes the form

$$\dot{u} = -\epsilon \nabla \Phi(y)^T = -4\epsilon y(y^2 - 1).$$

Figure 4 shows trajectories of the closed-loop system (3) for the same initial condition, but different

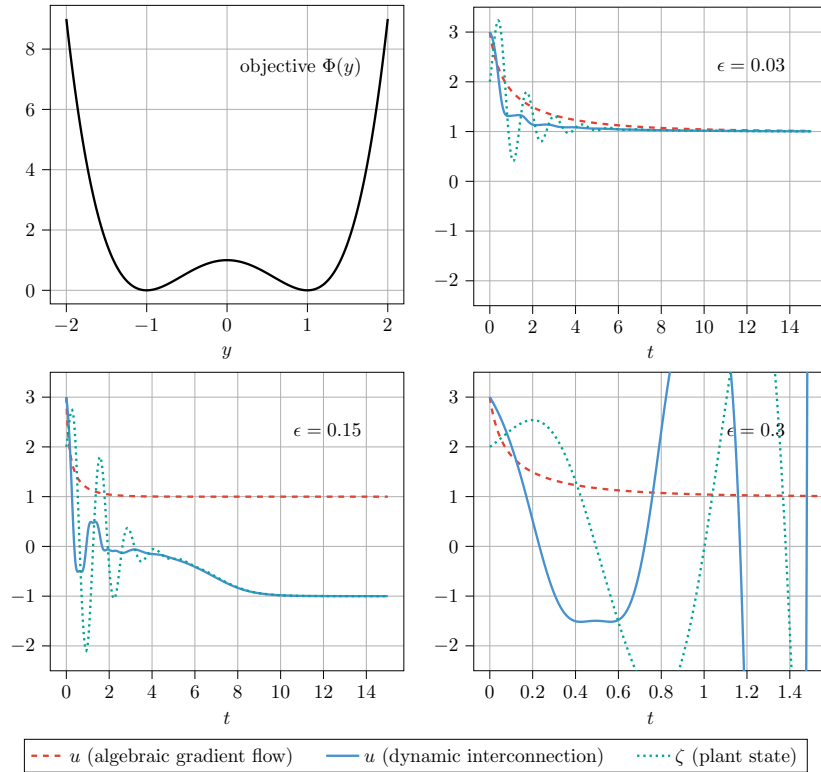


**Figure 4:** An illustration of the dynamic closed loop behavior when a gradient flow is interconnected with a stable physical plant (top left: objective function; remaining panels: system trajectories for different control gains  $\epsilon$ )

values of the gain  $\epsilon$ , and comparing it to the “algebraic” gradient flow (2) given by  $\dot{u} = -\epsilon \nabla \Phi(h(u))^T = -4\epsilon u(u^2 - 1)$ .

We observe, that for the given initial condition the algebraic gradient trajectory converges to the minimizer at 1. In contrast, the trajectories of the closed-loop system (3) converge to either one of the two minimizers or diverge, depending on  $\epsilon$ . In other words, closed-loop stability of (3) is not guaranteed, and even if it is, convergence may not be to the same minimizer as for (2).

This example illustrates that a simple gradient-based controller interconnected with a dynamical system is not necessarily stable, unless the control gain  $\epsilon$  is small enough. In other words, *sufficient timescale separation* between the fast plant behavior and the slow optimization dynamics is generally required. This approach is very general and applicable to nonlinear (but asymptotically stable) plant dynamics and non-convex optimization dynamics, but potentially very conservative.

Following up on the same example, let us characterize the stability of the feedback loop introduced before. In particular, we want formulate conditions on the gain  $\epsilon$  in Figure 2 that guarantee closed-loop stability. For this purpose we pass to the singular perturbation decomposition into reduced and boundary-layer error dynamics illustrated in Figure 5 [9]. In particular,  $\hat{h}$  is defined such that  $f(\hat{h}(u), u) = 0$  for all  $u$ .

The resulting reduced dynamics correspond exactly to the simplified model what we have already used in the design of the optimizing controller, where the plant is replaced by its algebraic steady-state map. The boundary-layer error dynamics  $z := \zeta - \hat{h}(u)$  evolve as  $\dot{z} = f(\zeta, u)$  for any fixed  $u$ . If these error dynamics are exponentially stable (and other technical assumptions are satisfied), standard converse results guarantee the existence of a Lyapunov function  $W$  and parameters  $\gamma, \omega > 0$  such that, for any





This conservatism of our bound is to be expected, especially considering the limited amount of information and computation required to evaluate  $\epsilon^*$ . Nevertheless, we consider  $\epsilon^*$  to be of practical relevance, in particular since the bound comes with the guarantee that for every  $\epsilon < \epsilon^*$  the interconnected system is asymptotically stable.

In Figure 6 we show the simulation results over a time span of 300 s in which the feedback controller tries to track the solution of a standard DC OPF problem under time-varying loads, i.e., non-constant disturbance  $w(t)$ . The optimal cost of this *instantaneous* DC OPF problem is illustrated in the first panel of Figure 6 by the dashed line. The minor violation of line and frequency constraints observed in the simulation is a consequence of control design that is based on soft constraints.

Additionally, we simulate the effect of a generator outage at 100 s and a double line tripping at 200 s. Both of which do not jeopardize overall stability. Furthermore, we do not update the steady-state map  $H$  after the grid topology change caused by the line outages. Nevertheless, the controller with the inexact model achieves very good tracking performance as illustrated in the first panel of Figure 6.

Overall, this simulation shows the robustness of feedback-based optimization against i) underlying dynamics, ii) disturbances in the form of load changes, and iii) model inaccuracy in the form of topology mismatch.

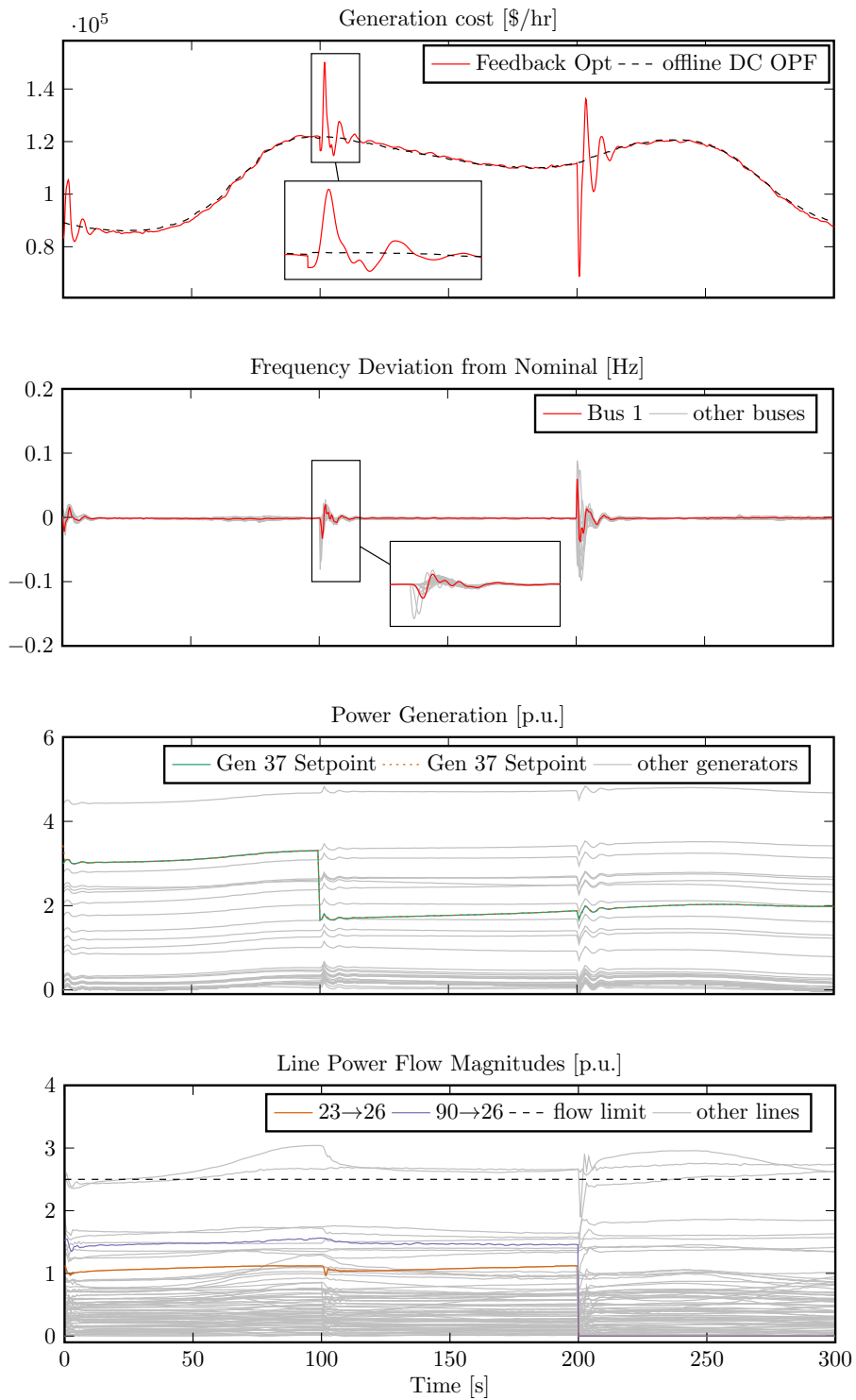


**Figure 6:** Simulation results for the IEEE 118-bus test case. An outage of a 200 MW generation unit happens at 100 s (producing approx. 175 MW at the time of the outage) and results in the loss of half the generation capacity at the corresponding bus (the bus power injection is highlighted in the third panel). A double line tripping happens at 200 s (the corresponding line power flows are highlighted in the fourth panel).

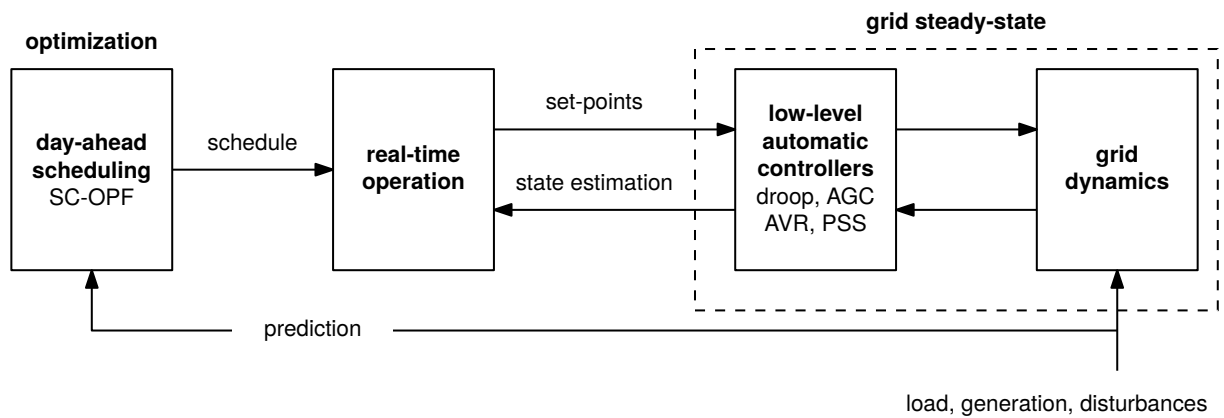


**Figure 7:** Schematic representation of the decision and control stages in power system operation.

## 3.2 WP2 Real-time power system operation

### D2.1 Power system operation scenarios

Power systems are operated through decision and control processes that happen at different time scales, as represented in Figure 7:

- At the slowest time scale lies an optimization stage: the operation of the grid is scheduled ahead of time based on predictions of the load and of the availability of generators, in order to minimize generation cost while ensuring sufficient resilience of the system against unforeseen events;
- At the fastest time scale, low-level automatic controllers ensure that the system tracks the given set-points; most of these controllers are local feedback controllers located at the generators.
- *Real-time operation* describes the interface between the aforementioned stages: set-points are generated in real-time based on the precomputed schedules and on the current state of the system, often made available via a state estimator.

The goal of the real-time operation stage is to follow the predetermined schedule as closely as possible while ensuring that the system state satisfies the operational constraints of the grid.

We have identified three specific real-time operation scenarios that focus on specific choices of the services to be automated, the set-points that can be actuated, the performance metrics, and the available measurements.

The proposed scenarios include both testbeds in the transmission grid and in the distribution grid, although the concept of real-time operation in the latter ones is not an accepted paradigm yet. We deliberately did so in order to explore the potential of these methods for the integration of Active Distribution Networks (ADNs).

### UNICORN-4 Cooperative Volt/VAR in power distribution grids

One important concern in the presence of distributed renewable generation is the occurrence of over-voltages in distribution feeders, which may force the distribution system operator to curtail generation. In this scenario, we consider the problem of controlling the voltage of a distribution feeder using the reactive power capabilities of the power inverters of the microgenerators. Control of reactive power flows is a relatively inexpensive way to regulate the feeder voltage and should therefore be fully exploited before resorting to these extreme remedial actions on the active power flows in the grid.

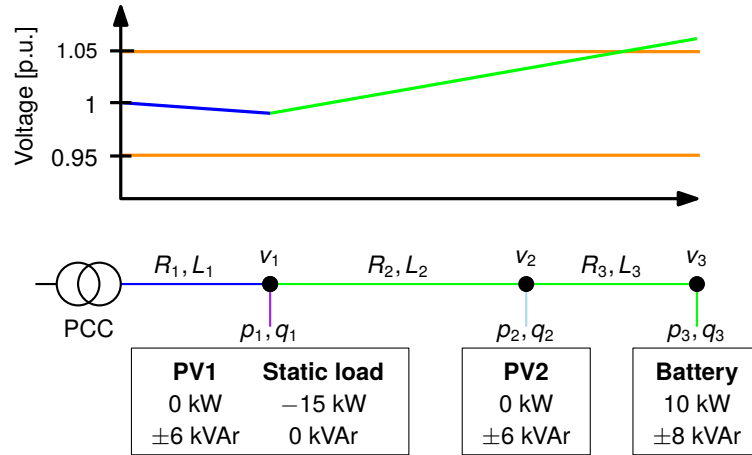


**Figure 8:** 4-bus test feeder proposed as a testbed for the “Cooperative Volt/VAR” scenario. Sketch of the voltage profile and of the distribution feeder topology.

$R_1$ [ $\Omega$ ]	$L_1$ [ $\Omega$ ]	$R_2$ [ $\Omega$ ]	$L_2$ [ $\Omega$ ]	$R_3$ [ $\Omega$ ]	$L_3$ [ $\Omega$ ]
0.195	0.124	0.11	0.027	0.97	0.093

**Table 1:** Cable parameters for the 4-bus test feeder in Figure 8.

**Testbed** We propose a small yet realistic distribution feeder where it is possible to observe an over-voltage condition caused by local generation. Without proper reactive power control, the feeder’s ability to host renewable energy injections is limited and generation has to be curtailed.

The testbed is represented in Figure 8. It consists of a battery, two photovoltaic panels (PV), a resistive static load, and the distribution substation (PCC) connecting the distribution feeder to the grid. The different nodes are connected via cables with non-negligible resistance (see Table 1).

The active power injection  $p_3$  of the battery represents a renewable source, which should not be curtailed. The local demand of the static load is larger than the local production, therefore a positive active power flow from the substation is required. The feeder voltage profile with no reactive power flows and no active power injection of the PVs is represented in Figure 8, where the overvoltage at the end of the feeder is apparent.

**Actuation** The reactive power injection of the PVs and of the battery can be controlled, up to the limits reported in Figure 8.

**Sensing** Both the PVs and the battery can measure the voltage magnitude at their point of connection.

**Operational constraints** The voltage limits are defined to be 0.95 p.u. and 1.05 p.u.

**Performance metric** Fair reactive power sharing (i.e., proportional use of the reactive power capability of each inverter) is the measure of performance.

**Benchmark experiment** We consider the case in which PV panels are not injecting any active power, and the battery is injecting constant active power. As reported in Figure 8, this setup yields an overvoltage condition.



**Purpose** This benchmark experiment was chosen because it constitutes a Volt/VAr regulation problem which cannot be solved without a coordinated control strategy like the ones currently employed in real-time operations [11, 12, 13] (see the simulation results in D2.2 and the experimental results in D3.2).

At the same time, the testbed is extremely simple. The global optimum of the Volt/VAr regulation problem can be certified, as also the suboptimality of any completely decentralized control strategy (see [14]). The simple step-like exogenous disturbances allow to analyze the transient behavior and to assess the rate of convergence.

Moreover, the exact topology is available at the SYSLAB infrastructure at DTU Risø, Denmark, where the benchmark experiment can be implemented on a real distribution feeder (see D3.2).

**Data availability** This testbed has been used in two journal publications [15, 16]. The public UNICORN project repository will contain

- test feeder topology and data,
- the corresponding MATPOWER test file,
- reproducible simulations for standard Volt/VAr control schemes, and
- instructions for experimental validation at the SYSLAB infrastructure.

### **UNICORN-56 Optimal generation curtailment in power distribution grids**

This scenario is qualitatively similar to the previous scenario, as it is also motivated by overvoltage in power distribution grids caused by distributed renewable generation. In this scenario, however, both active and reactive power injection of the distributed generators can be controlled, and the ultimate goal is to reduce the total amount of energy curtailed over an extended period of time.

**Testbed** As a testbed, we adopted the test feeder used in [17, 14] and consisting in the three-phase backbone of the standard IEEE 123-bus distribution test feeder [18]. The resulting 56-bus feeder is schematically reported in Figure 9.

**Actuation** The active and reactive power injection of the two microgenerators can be controlled. The upper limit to the active power injection is time-varying, as it depends on the available primary source (solar irradiation). Reactive power limits depend on the inverter sizing, and possibly on the simultaneous active power injection.

**Sensing** Both the microgenerators can measure their voltage magnitude.

**Operational constraints** The overvoltage limit is set to 1.05 p.u.

**Performance metric** The measure of performance is the total net balance of renewable energy production (injected active power minus power losses).

**Benchmark experiment** We consider the behavior of the grid over a time window of 12 hours.

The power demand of each bus during this time window is obtained by aggregating the power demand profiles available in the DiSC simulation framework [19]. They represent the power consumption of about 1200 individual households from the area around the Danish city Horsens, obtained as anonymized data



**Figure 9:** The 56-bus feeder proposed as a testbed for the “Optimal generation curtailment in power distribution grids” scenario.

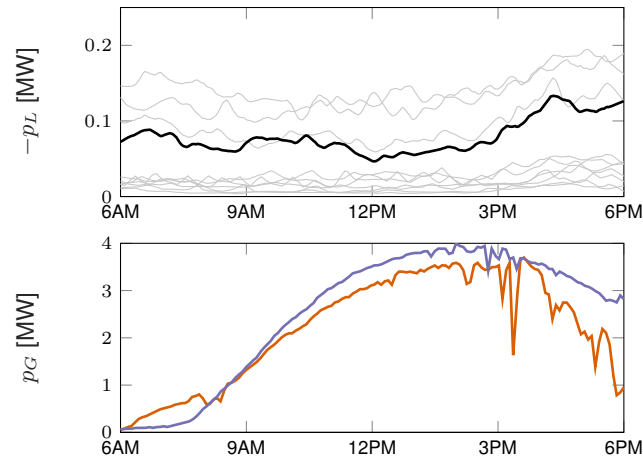


**Figure 10:** Power generation and power demands for the 56-bus testbed reported in Figure 9.

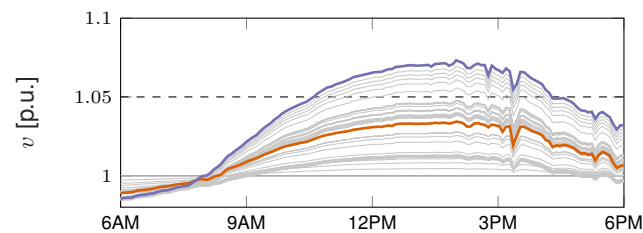


**Figure 11:** Overvoltage of the 56-bus test feeder caused by the power generation and demand reported in Figure 10.

from the Danish DSO NRGi. The resulting power demand profiles for a 12-hour period (6 AM to 6 PM) have been plotted in Figure 10, where one profile has been highlighted as an example.

The upper active power limit for the two microgenerators describes a typical solar irradiance pattern, and is also reported in Figure 10.

Under these conditions, no reactive power control and no curtailment will yield an overvoltage condition (Figure 11).

**Purpose** This benchmark represents a typical curtailment problem in a distribution grid with limited power transfer capacity. The focus of the benchmark is the average curtailment in a dynamic setup, in which both loads and active power generation are time-varying. The realistic consumption and production data allow to assess the effect of the dynamic performance of real-time operations on the overall energy efficiency.

**Data availability** This testbed has been used in a journal paper appeared in the IEEE Transactions on Control of Network Systems [14] for a simpler Volt/VAr control problem. The corresponding code is currently available online [20, 21].

The public UNICORN project repository already hosts

- test feeder topology and data,
- the corresponding MATPOWER test file,
- time series data for power generation and demand (with permission of the respective owners).

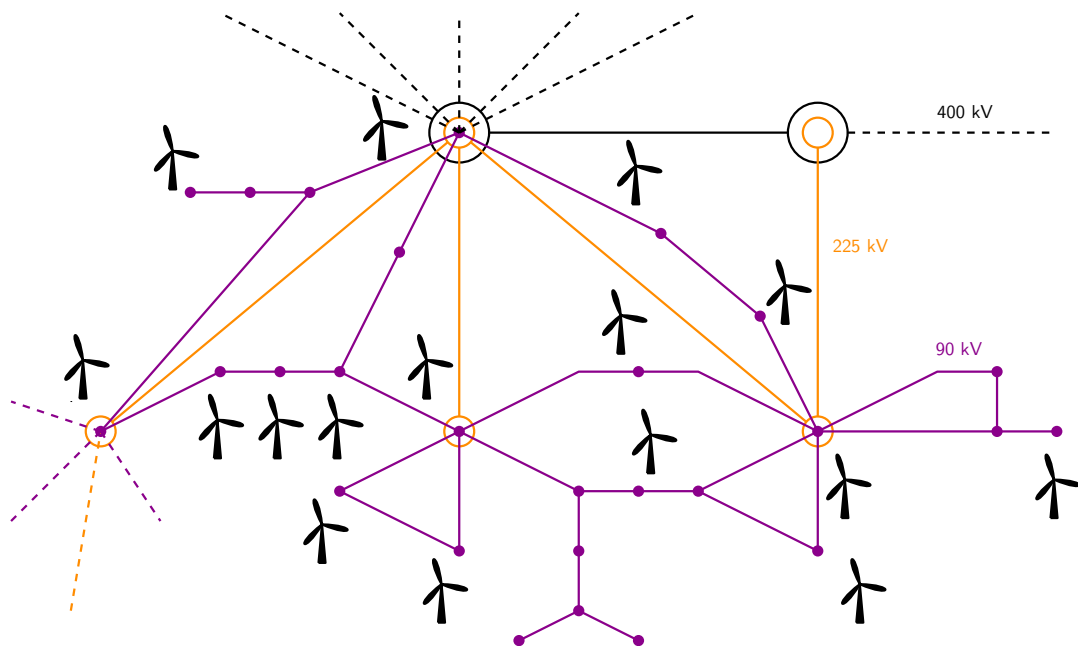


**Figure 12:** The Blocaux area (benchmark UNICORN-7019) with 42 wind farms, 31 buses, and 58 branches. Connections to the rest of France are indicated with dashed lines.

### UNICORN-7019 Subtransmission congestion relief

The installation of a large number of medium-size generators poses unprecedented challenges in terms of congestion (overvoltage, line capacity violation) of the subtransmission grid where these generators are connected. Curtailment of these renewable sources can be avoided or minimized by exploiting multiple control actions, such as reactive power compensation by the same generators and tap changers control.

**Testbed** The grid model for the benchmark is the real French transmission grid system, which consists of 7019 buses, 9657 branches, 1465 generators, and 907 tap changers. We consider a 31-bus portion of the French grid (area of Blocaux, Figure 12) that includes a 63kV subtransmission network and a 225kV transmission network. 20kV distribution feeders are connected to the 63kV grid. Some 20kV feeders in the area hosts multiple 12 MW wind farms.

The installed wind power exceeds the capacity of the grid and during the summer of 2021 the wind farms were curtailed at a fixed level of 70% of their installed power to prevent overloaded lines.

The task in the benchmark is to minimize the losses and active power curtailment in the Blocaux area using the active and reactive power injections of the wind farms and the on-load tap changers, while satisfying the grid constraints, i.e. voltage magnitude limits at the buses and power flow limits on the lines. During the simulation the wind power produced by the wind farms is changing, see Figure 13.

**Actuation** The following control actions are available:

- Power generation from renewable sources (wind) in the 20kV network can be curtailed/modulated. Curtailment signal is forwarded by DSOs.
- The reactive power injection of the generators in the 20kV network can be controlled.
- Some tap changers between the 63kV grid and the 225kV and a few of those between the 20kV grid and the 63kV grid can be controlled. If uncontrolled, tap-changers obey local prescribed control laws.

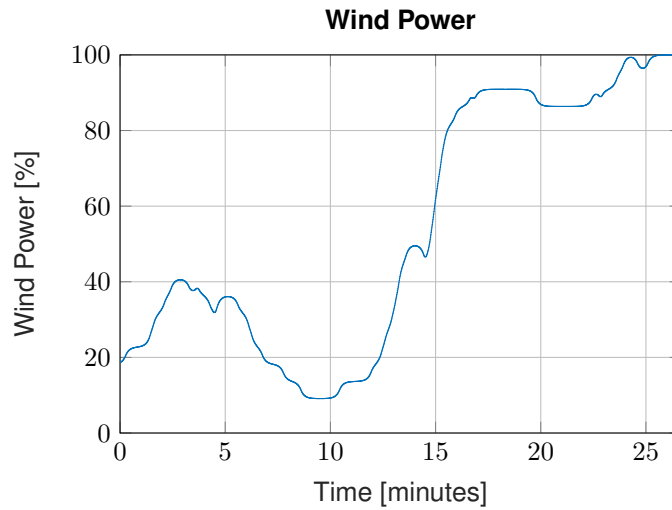


**Figure 13:** Wind profile with fast increase from 20% to 90% within 5 minutes.

**Sensing** The entire electric state of the 90 kV network (and higher) is measured: active/reactive power flows, voltage magnitudes, and currents. A typical sample rate is 1 measurement/second.

**Operational constraints** Subtransmission grid congestion is defined, for the purpose of this testbed, as the violation of overvoltage limits or of line power ratings.

**Performance metric** The goal of real-time operation in this testbed is to minimize the curtailment or renewable energy sources.

**Benchmark experiment** The benchmark experiment will include a fast increase in active power injection by the wind generators. Overvoltage and line overload will be observed if no remedial actions take place, also due to the relatively low power demand of the loads (summer period).

**Purpose** This benchmark represents a real grid congestion problem that needs to be tackled via the coordinated control of multiple heterogeneous actuators towards the same goal. The overall performance is expected to depend on how well these resources are coordinated. Compared to the previous scenarios, this testbed represents a zonal control problem in a highly interconnected grid rather than a separated system.

**Data availability** The data that constitute this benchmark have not been made public by RTE before this project. The public UNICORN project repository will contain

- test feeder topology and data,
- the corresponding MATPOWER test file,
- a Matlab toolbox to integrate tap changers in MATPOWER simulations,
- reproducible numerical experiments.



	UNICORN 4-bus	UNICORN 56-bus	UNICORN 7019-bus
<b>Scenario</b>	Cooperative Volt/VAR in power distribution grids	Optimal generation curtailment in power distribution grids	Subtransmission congestion relief
<b>Domain</b>	distribution	distribution	transmission
<b>Dimension</b>	4 buses	56 buses	31 buses of the 7019-bus French grid
<b>Actuation</b>	reactive power	generation curtailment reactive power	generation curtailment reactive power tap-changers
<b>Sensing</b>	generator voltage	generator voltage	full transmission grid state
<b>Operational constraints</b>	voltage limits	voltage limits	voltage limits line flow limits
<b>Performance metric</b>	satisfaction of voltage limits	satisfaction of voltage limits curtailment minimization	satisfaction of voltage limits satisfaction of line flow limits curtailment minimization losses minimization
<b>Benchmark</b>	static scenario	time-varying scenario	time-varying scenario

**Table 2:** Summary of the three proposed scenarios.

## D2.2 Real-time power system operation

We now briefly illustrate the application of the proposed real-time control methodologies in the three scenarios identified in D2.1. While we keep the presentation relatively brief here and we present only the most important highlights, we refer to the project open-access publications for an in-depth analysis of each of them.

### UNICORN-4 Cooperative Volt/VAR in power distribution grids

The real time control problem presented in the UNICORN-4 benchmark can be abstracted as follows. Determine the reactive power  $q_h$  at every DER  $h$  such that  $q_{\min} \leq q_h \leq q_{\max}$  and that  $v_{\min} \leq v_h(q, w) \leq v_{\max}$ . Here,  $v_h(q, w)$  is the steady state map of the nonlinear power flow equations that defines voltages  $v_h$  as a function of both reactive powers  $q_h$  and external influences  $w$  (e.g., active and reactive demands, active generation). Mathematically speaking, we try to solve a feasibility problem:

$$q \in \mathcal{F} \quad \mathcal{F} := \{q \mid q_{\min} \leq q \leq q_{\max}, v_{\min} \leq v(q, w) \leq v_{\max}\},$$

where  $q$  and  $v$  are the vectors of reactive power set-points and voltage magnitudes that we obtain by stacking the individual  $q_h$  and  $v_h$  of the DERs, respectively. In order to apply the proposed methodology, we cast this feasibility problem into the optimization problem

$$\begin{aligned} \min_q \quad & \frac{1}{2} q^T M q \\ \text{subject to} \quad & v_{\min} \leq v_h(q, w) \leq v_{\max} \quad \forall h \\ & q_{\min} \leq q_h \leq q_{\max} \quad \forall h \end{aligned} \quad (12)$$

where  $M$  can be used to weight the reactive power contribution of the different inverters  $h$ .

As prescribed by the approach presented in D1.1, we select an iterative optimization algorithm that we want to “translate” into a feedback controller. In this case, we selected a *dual ascent flow* (see [15] for the detailed derivation).

We introduce the dual variables  $\lambda_{\min}$  and  $\lambda_{\max}$  corresponding to the voltage (output) constraints. We obtain the dual updates

$$\lambda_{\min}(t+1) = [\lambda_{\min}(t) + \alpha(v_{\min} - v)]_{\geq 0} \quad (13)$$

$$\lambda_{\max}(t+1) = [\lambda_{\max}(t) + \alpha(v - v_{\max})]_{\geq 0}. \quad (14)$$

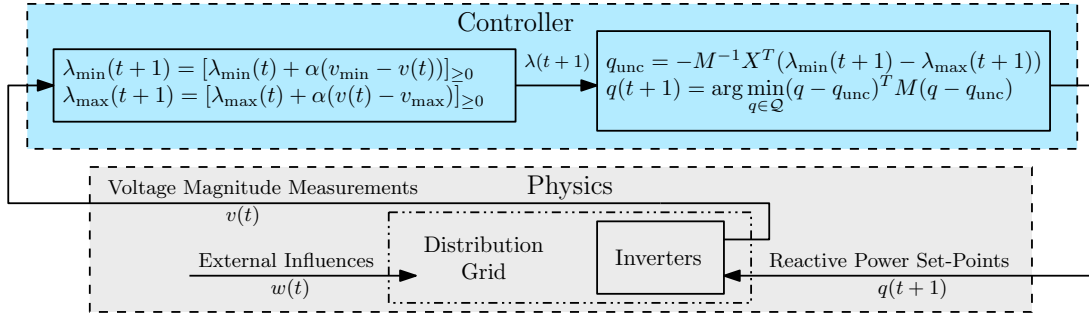


**Figure 14:** Block diagram of the controller with (13) and (14) (left block) and (16) and (17) (right block). The controller gets the voltage magnitude measurements from the inverters and determines the reactive power set-points, which are send to the inverters. The parameter  $\alpha$  is the controller gain and is the only tuning knob. Note, that the left block corresponds to the integral part of a PI-controller.

As we can see, we are integrating the voltage violations, which can be measured, with a gain of  $\alpha$ .

As discussed in D1.1, in order to perform the primal update step (minimization in the primal variables), we need an approximation of the sensitivity of the voltages with respect to the reactive power injection akin to power transfer distribution factors for active power generation on the transmission level. Under no-load conditions and the assumption of negligible cable resistances we have the approximation

$$\frac{\partial v(q, w)}{\partial q} = X, \quad (15)$$

where  $X$  is the reduced bus reactance matrix that can be derived from the grid topology and the power line/cable data. The approximation is accurate for lightly loaded systems, because the nonlinearity of the power flow equations is mild near this operating point [6]. In our application the system can be heavily loaded, but we verify that the proposed FO is sufficiently robust against this model mismatch.

The the optimal unconstrained reactive power set-points  $q_{\text{unc}}$  becomes

$$q_{\text{unc}} = M^{-1} X^T (\lambda_{\min}(t+1) - \lambda_{\max}(t+1)), \quad (16)$$

while the solution of the constrained optimization problem becomes

$$q(t+1) = \arg \min_{q \in \mathcal{Q}} (q - q_{\text{unc}})^T M (q - q_{\text{unc}}), \quad (17)$$

where  $\mathcal{Q} = \{q \mid q_{\min} \leq q \leq q_{\max}\}$ .

In practice, these reactive power set-points  $q(t+1)$  are to be communicated to the different DERs, which will adjust their reactive power accordingly and collect the measurement of the consequent steady state voltage magnitudes, which need to be communicated to the central control unit. Therefore, at every time step the measurement and set-point need to be communicated by and to every inverter, respectively. The resulting centralized controller is represented in Figure 14 and consists of equations (13) and (14) (left block in the figure) and (16) and (17) (right block in the figure).

We can see that the FO controller uses the same measurements as local controllers, but these measurement are processed by a central unit which coordinates the actions of the different DERs and steers the system to the optimal steady state. In comparison to the OPF-based dispatch, no nonlinear model nor knowledge of the power consumption or generation (modeled as external influences  $w$ ) is needed.

This controller has been experimentally validated in the SYSLAB distribution grid at DTU Risø, Denmark. The UNICORN-4 benchmark has been replicated on a configurable distribution feeder, with the line parameters summarized in Table 3. The resulting physical topology is reported in Figure 15 and in Table 4. The same setup was used in [16] to analyze a distributed FO controller for the Volt/VAR problem. Without proper reactive power control, the feeder's ability to host renewable energy injections is limited



**Table 3:** Overview of the resistances and inductances in the grid.

$R_1$ [ $\Omega$ ]	$L_1$ [ $\Omega$ ]	$R_2$ [ $\Omega$ ]	$L_2$ [ $\Omega$ ]	$R_3$ [ $\Omega$ ]	$L_3$ [ $\Omega$ ]
0.195	0.124	0.11	0.027	0.97	0.093

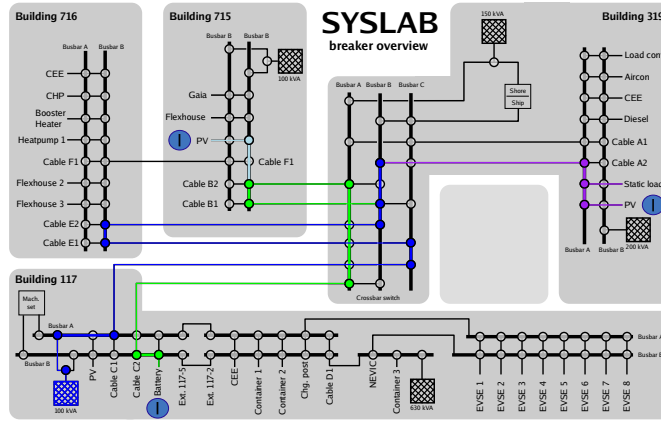


**Figure 15:** Implementation of the 4-bus testbed at the SYSLAB facility at DTU, Denmark. The colors of the cables correspond to the colors of the diagram in Figure 8.

and generation has to be curtailed. This scenario was chosen because it constitutes a non-trivial voltage regulation problem which cannot be solved without a coordinated Volt/VAr control strategy.

The setup consists of a vanadium battery, two photovoltaic systems (PV), a resistive load, and the distribution substation (PCC) connecting the distribution feeder to the remaining grid, see Figure 8. The different nodes are connected via cables with non-negligible resistance (Table 3). The cable connecting the battery to the grid has a particularly large resistance.

The active power injection  $p_3$  of the battery can represent a renewable source, which should not be curtailed. In our experiments we choose the active power of the battery to be  $p_3 = 10$  kW. The high cable resistance and active power injection deteriorates the approximation of the sensitivity matrix in (15). The static load is set to an active power consumption of 15 kW ( $p_1 = -15$  kW) which is larger than the local production, therefore requiring a positive active power flow from the substation. PVs are fluctuating power sources. Therefore, to facilitate repeatability of the experiments and to allow for a comparison between different controllers, the PVs do not inject active power ( $p_2 = 0$  kW).

The resulting voltage profile with no reactive power flows is represented in Figure 8, where the overvoltage at the end of the feeder is apparent.

Both the PVs and the battery can measure their voltage magnitudes, and their reactive power injections can be controlled. The PV inverters have a reactive power range of  $\pm 6$  kVar and the battery can be actuated with  $\pm 8$  kVar. The inverters at SYSLAB are oversized such that their full reactive power range is available independently of their concurrent active power injection. The PVs and the battery can communicate with a central computational unit via a general-purpose Ethernet network, while the load is uncontrolled and unmeasured.

The voltage limits are defined to be 0.95 p.u. and 1.05 p.u. We set these limits tighter than most grid codes in order to be able to observe persistent overvoltages without hardware protections being activated.

The FO controller is implemented in Matlab at a central computation unit (Figure 14), where it is provided with the voltage magnitude measurements from the different inverters and computes the reactive power set-points. These are sent to the inverters every 10 seconds, because the PV systems in the laboratory were not to be actuated more frequently, due to special hardware constraints. In general, the controller



Cable	Length [m]	Cross Section [mm <sup>2</sup> ]	R [ $\Omega$ ]	X [ $\Omega$ ]
A2	25	95	0.0078	0.002
B1 & B2	350	95	0.11	0.027
C1 & C2	700	240	0.085	0.054
E1 & E2	450	240	0.055	0.035
PV1	83	16	0.095	0.007
PV2	8	6	0.025	0.0008
Battery	100	2.5	0.774	0.012
Static Load	11	95	0.002	0.001

**Table 4:** Overview of the cables connecting the busbars and the devices to the busbars.

can run more frequently.

We implement a local droop controller and an OPF-based dispatch as two benchmark solutions to compare with the proposed FO strategy. These approaches have almost opposite features: The droop controller only needs local voltage magnitude measurements, no communication, and no model of the grid; the OPF-based dispatch is centralized, requires communication of full state measurements (all power generation and demand), and relies on an accurate nonlinear grid model.

We repeat the following 21-minute experiment for the three aforementioned strategies: droop control, OPF-based dispatch, and FO.

- All power inverters are initialized with zero reactive power injection.
- After three minutes the controllers are activated and start regulating the voltage.
- After 11 minutes the active power injection of the battery is reduced to 0 kW (effectively removing the cause of the overvoltage and the need for reactive power regulation).
- At minute 14 the active power injection is stepped up again to 10 kW for the remaining 7 minutes of the experiment.

The droop controller that we implement complies with the recommendations by recent grid codes [13, 12, 11]. Every DER measures the magnitude of the voltage at their point of connection and absorbs/injects reactive power following a piecewise linear control law.

The performance of the *droop controller* can be seen in Figure 16a. Once the controller is activated the reactive power of the battery drops to its lower limit which reduces the overvoltage. However, the limited reactive power capability of the battery cannot drive the voltage into the desired voltage range. The PV systems do not absorb reactive power to help reduce the overvoltage because they do not sense an overvoltage condition at their point of connection, and they will not lower their voltage below the nominal value of 1 p.u. This behavior is general for all local control strategies, and cannot be prevented without introducing some form of coordination between the inverters. Local control strategies are therefore inherently suboptimal; as established from a theoretical perspective in [14].

We implement an *OPF-based dispatch* by communicating all reactive and active power consumption and generation to a centralized computation unit. There, we solve (12) using an OPF solver, which uses a nonlinear grid model that we obtain from the grid topology and the data from Table 3. The reactive power set-points which are the solution of (12) are then given to the inverters. This approach guarantees optimality of the set-points under perfect model knowledge, but all power generation and consumption needs to be measured or estimated. This information is available at SYSLAB with a significant level of accuracy. In most distribution grids, the cable data and grid topology are not known exactly, nor are all reactive and active power consumption and generation measurements available. Nevertheless, because of model mismatch, the OPF solution does not lead to feasible voltages (see the persistent voltage violation in Figure 16b).

Finally, we have implemented the proposed Feedback Optimization algorithm on the same benchmark. The control performance can be seen in Figure 16c. When the controller is activated the central unit is

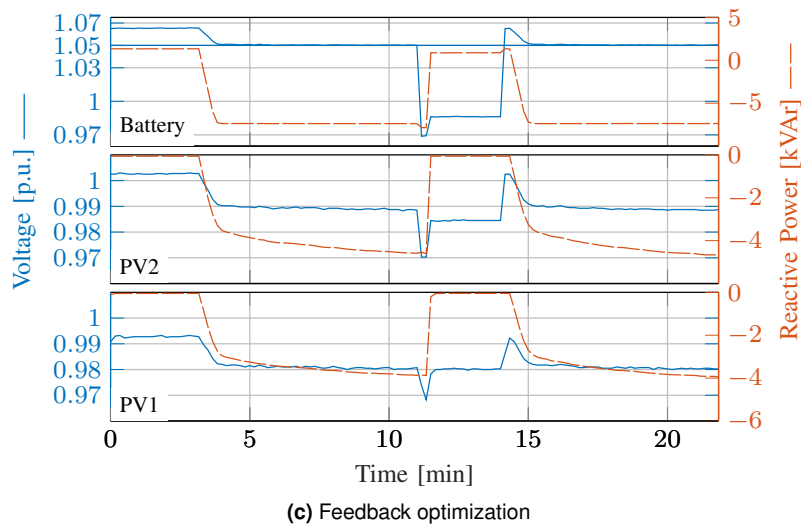
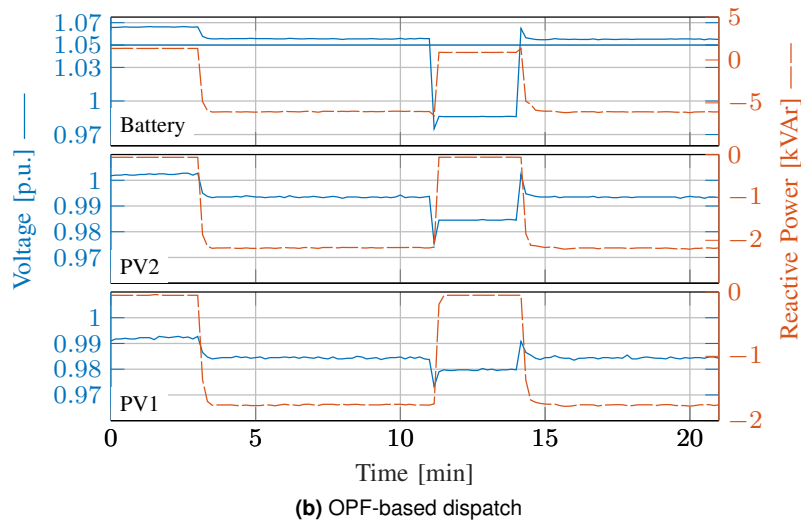
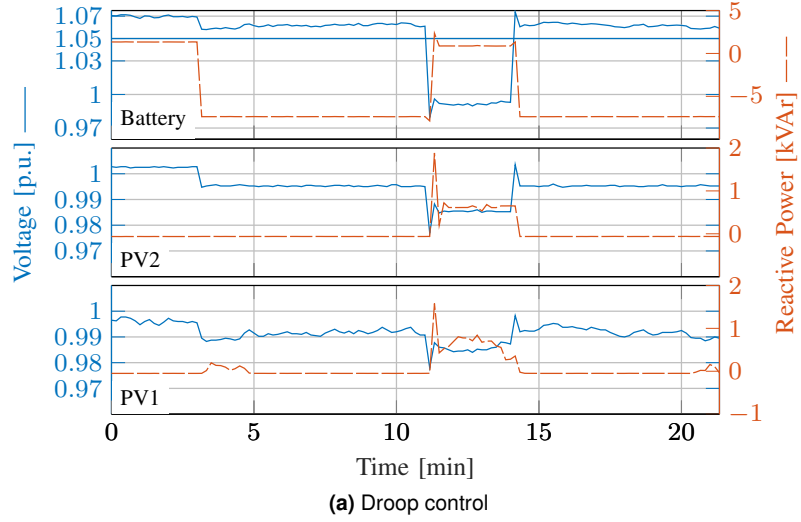


Figure 16: Performance of different control schemes on the UNICORN-4 benchmark.



provided with the voltages at the PV systems and the battery. The dual variable  $\lambda_{\max,3}$  that corresponds to the violation of the upper voltage limit of the battery starts integrating the violation. This then leads to all inverters reducing their reactive power injections. As long as there is an overvoltage the dual variable keeps integrating, which leads to the inverter absorbing more reactive power which lowers the voltage. At steady state the voltage at the battery is at the upper voltage limit and the reactive power injections are at the optimal solution of (12).

In conclusion, we have experimentally demonstrated that the proposed FO strategy outperforms industrial standards and OPF-based approaches, and drives the system to the feasible voltage range while relying only on voltage measurements collected from the inverters (without measuring or estimating any power flows). Within our experimental setup, feedback optimization is extremely robust to model mismatch and its design and tuning is essentially model-free (see details in [15]).

### UNICORN-56 Optimal generation curtailment in power distribution grids

As discussed in D2.1, the UNICORN-56 benchmark is a distribution voltage control problem that is substantially similar to the UNICORN-4 benchmark, with two important differences:

- active power curtailment is possible (and it is in fact needed to prevent overvoltage)
- the time-varying generation and demands (see Figure 10) allow to test the dynamic performance of the feedback controllers.

The resulting overvoltage contingency is illustrated in Figure 11, where it is clear that the voltage magnitude exceeds the limit of 1.05 p.u. in multiple buses.

The derivation of the feedback optimization controller for this applications follows the same steps that we presented to the UNICORN-4 benchmark, but applied to the following optimization problem instead of (12):

$$\begin{aligned} \min_{p,q} \quad & \frac{1}{2}q^T q + \frac{1}{2}(p - p_{\text{MPPT}})^T(p - p_{\text{MPPT}}) \\ \text{subject to} \quad & \leq v_h(p, q, w) \leq v_{\max} & \forall h \\ & p_{\min} \leq p_h \leq p_{\max} & \forall h \\ & q_{\min} \leq q_h \leq q_{\max} & \forall h. \end{aligned} \quad (18)$$

Notice that the cost function includes a penalty on the difference between the active power injection of the PV panels and the maximal power injection  $p_{\text{MPPT}}$  that they could deliver, given the current solar irradiation conditions. Notice also that in this case the distribution feeder is preventively designed so that undervoltage cannot occur, so we only include an overvoltage constraint in the real-time optimization problem.

As before, the proposed controller (available in the public project repository) alternates between a gradient step in the dual variables and an exact minimization step in the primal variables (in this case,  $p$  and  $q$ ).

The dual update step, which basically corresponds to an integral update of the internal states  $\lambda$  of the controller, take the form

$$\lambda(t+1) = [\lambda(t) + \alpha(v - v_{\max})]_{\geq 0}. \quad (19)$$

In order to compute the primal minimization step, we implement, at each iteration of the measurement-actuation cycle, a series of  $K$  gradient descent steps in the primal variables. This correspond to an inexact minimization in the primal variables, although with a number of iterations as low as  $K = 10$  the remaining suboptimality is minimal.

To implement this, the controller is also equipped with an internal state  $\hat{p}$  and  $\hat{q}$  that stores the temporary values of the set-points before they are sent to the power converters. Each of the  $K$  “inner” steps



corresponds to the updates

$$\begin{aligned}\hat{p}(k+1) &= [\hat{p}(k) - \gamma R(\hat{p}(k) - p_{\text{MPPT}} + \lambda(t))]_{p_{\text{min}}}^{p_{\text{max}}} \\ \hat{q}(k+1) &= [\hat{q}(k) - \gamma X(\hat{q}(k) + \lambda(t))]_{q_{\text{min}}}^{q_{\text{max}}}\end{aligned}\quad (20)$$

initialized at

$$\begin{aligned}\hat{p}(0) &= p(t), \\ \hat{q}(0) &= q(t).\end{aligned}\quad (21)$$

A few remarks are due.

- Also in this case the controller does not need accurate model information about the grid, but only input-output sensitivities. In particular, the sensitivity between changes in active power (respectively, reactive power) and voltage magnitudes is needed. Although these sensitivities depend on the operating point of the grid, we replace them with the no-load sensitivities, who correspond, respectively, to the bus resistance and reactance matrices of the grid.
- By adopting a inexact minimization step in the primal variables, which is then implemented as a finite number of gradient descent steps, we show that the feedback optimization controllers can be implemented without resorting to any optimization solver, but relying only on simple algebraic manipulations of the inputs. This makes this approach feasible also for the deployment on embedded systems, including the onboard intelligence in consumer-level power converters.
- The algorithm includes two tunable parameters, the gains  $\alpha$  and  $\gamma$ . Their value affect the convergence speed of the algorithm and, possibly, its stability. A procedure to compute upper bounds for these parameters in order to guarantee stability of the controller is provided in [14].
- The number of steps  $K$  that need to be executed in order to approximate the solution of the primal minimization problem sufficiently well depends on the dimension on the problem, but it is typically low. A numerical experiment on the UNICORN-56 benchmark with larger number of microgenerators is reported in [16].

The resulting closed-loop behavior of the system is represented in Figure 17, where we allowed a time delay of 5 seconds between the update of set-points and the steady state of the voltages. It is clear that, via this control strategy, both agents successfully participate in the regulation of the voltage. Active power curtailment is also applied in order to maintain a feasible voltage, when reactive power does not suffice any more.

Notice also that the sudden change in solar irradiation that is included in the time series of the UNICORN-56 benchmark allows to test the dynamic performance of the proposed controller. The effect of that disturbance is visible in the brief overvoltage at around time 9.

### UNICORN-7019 Subtransmission congestion relief

The control objective in this benchmark is to use tap changers and wind farms (active and reactive power injections) to minimize the losses in the grid and to avoid active power curtailment as much as possible. Meanwhile, we have to satisfy the voltage constraints at all buses and the current constraints on all lines. To formalize this task as an optimization problem, we define the input as  $u = [q^T, p^T, tap^T]^T$  and the output as  $y = [v^T, i^T]^T$ . The cost function is the sum of power losses and curtailment costs. This

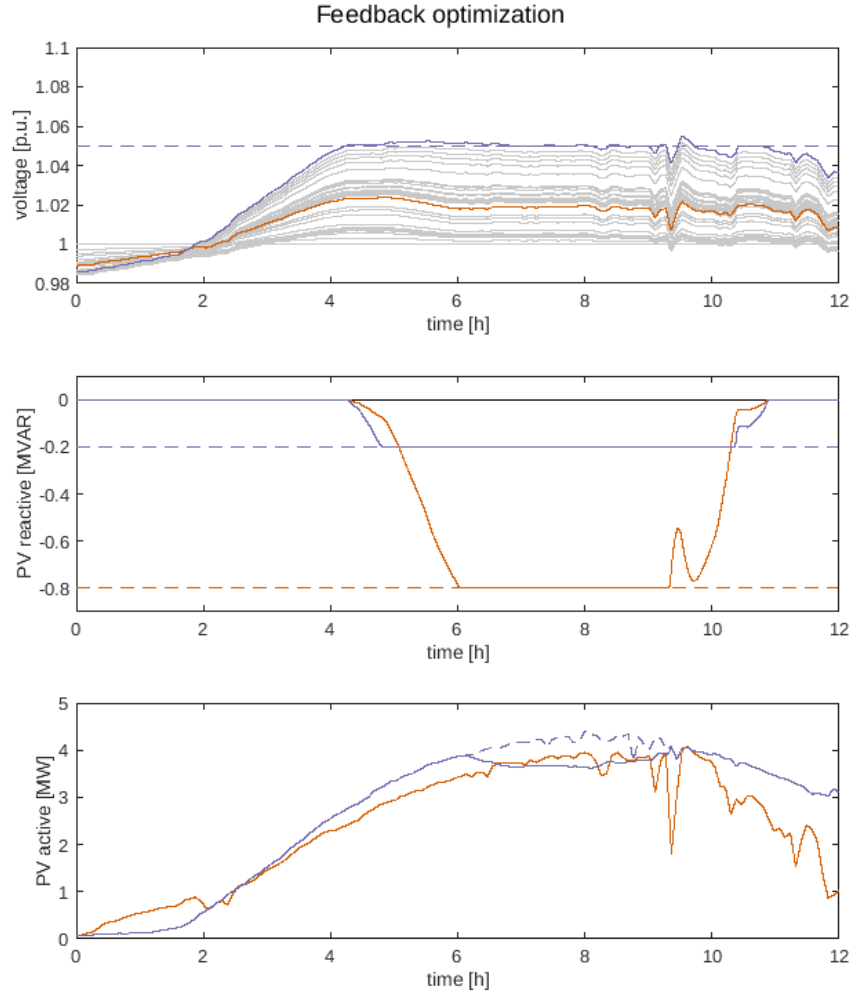


**Figure 17:** Simulation of the UNICORN-56 benchmark with the proposed feedback optimization controller.

leads to the optimization problem

$$\begin{aligned} \min_{u=[q,p,tap]} \quad & \text{losses}(u) + \text{curtailment}(u) \\ \text{s.t.} \quad & q_{min} < q < q_{max} \\ & p_{min} < p < p_{max} \\ & tap_{min} < tap < tap_{max} \\ & v_{min} < v(u) < v_{max} \\ & i_{min} < i(u) < i_{max} \end{aligned} \tag{22}$$

Compared to the optimization problems that we encountered in both the benchmarks UNICORN-4 and UNICORN-56, this benchmark is characterized by a higher number of constraints that need to be satisfied at any point in time. This feature affects the choice of the iterative optimization algorithm that we want to interconnect and use as a real-time controller, as primal-dual or dual-ascent algorithms, like those used in the two other benchmarks, tend to be harder to tune in the presence of multiple constraints and cannot prevent temporary violation of them (see the discussion in D1.1). For this reason, we opted for a projected gradient descent flow for this specific application. Compared to other optimization flows, projected gradient descent requires special care when it needs to be implemented in discrete time iterations. We quickly review the procedure here, and we refer to our work [22] for the technical details of this derivation.



Consider the general optimization problem

$$\begin{aligned} & \min_u f(u, y) \\ & \text{s.t. } y = h(u, d) \\ & \quad u \in \mathcal{U} \\ & \quad y \in \mathcal{Y}, \end{aligned} \tag{23}$$

of which (22) is a specific instance. A projected gradient iteration takes the form

$$u(k+1) = u(k) + \alpha \hat{\sigma}_\alpha(u(k), y_m) \tag{24}$$

with

$$\hat{\sigma}_\alpha(u, y_m) := \arg \min_{w \in \mathbb{R}^p} \|w + G^{-1}H(u)^T \nabla \Phi(u, y_m)^T\|_G^2 \tag{25}$$

$$\text{subject to } A(u + \alpha w) \leq b \tag{26}$$

$$C(y_m + \alpha \nabla h(u)w) \leq c, \tag{27}$$

where  $G$  is a weighting matrix with which the control gain can be adjusted. This is a convex quadratic optimization problem that is easy and fast to solve even for high dimensional settings.

Under standard assumptions on the well-posedness of the problem, we showed that [22, Theorem 3]

1. at the limit  $\alpha \rightarrow 0$  the iterative discrete-time update (24) converges to a continuous-time projected gradient flow;
2. for sufficiently small  $\alpha$  the trajectory of the closed loop system converges to the stationary points of the optimization problem (23);
3. if an input  $u^*$  is an asymptotically stable point for the closed loop system, then it is a strict local minimum for (23).

Figure 18 illustrates the main advantage of this optimization scheme compared to primal-dual or saddle flows. By taking sufficiently small values of  $\alpha$  it is possible to ensure stability of the closed loop system and, at the same time, to ensure that the trajectory of the system lies completely inside the feasible region.

Similarly to the other methods reviews in D1.1, the key model information that is needed is the sensitivity  $\nabla_u h(u, d)$ , which describes the effect of a change in the input on the output. The sensitivity  $\nabla_u h(u, d)$  depends on both  $u$  and  $d$  and on the system parameters, e.g. topology and line impedances. As discussed before, feedback optimization schemes are particularly robust with respect to model mismatch, therefore in this application it is possible to use a constant approximation of these sensitivities at the cost of a slight suboptimality of the steady state of the algorithm. In the context of the project we have also looked into methods to learn the sensitivity online from measurements, and we refer to [23] for a discussion of this approach.

When this method is applied to the subtransmission congestion control problem of the benchmark UNICORN-7019, we obtain the control architecture of Figure 19. Notice how the proposed architecture requires the presence of a communication channel that allows to both gather the state (or a state estimate) of the subtransmission grid, and to send updated set-points to all the controlled devices. Some of these set-point may have to be pre-processes (e.g., the tap changer positions) in order to comply with device specifications like ramp constraints, maximum frequency of updates, and quantization levels.

The effectiveness of the proposed approach can be appreciated from Figure 20. One can see how the system rides through the quick change in active power injection by the wind generators by activating different services, as different constraints become active.

In a first phase (until approx. 15 minutes) the wind generation is modest. Voltages across the entire area of the subtransmission grid are kept as high as possible (as long as they satisfy the constraints,

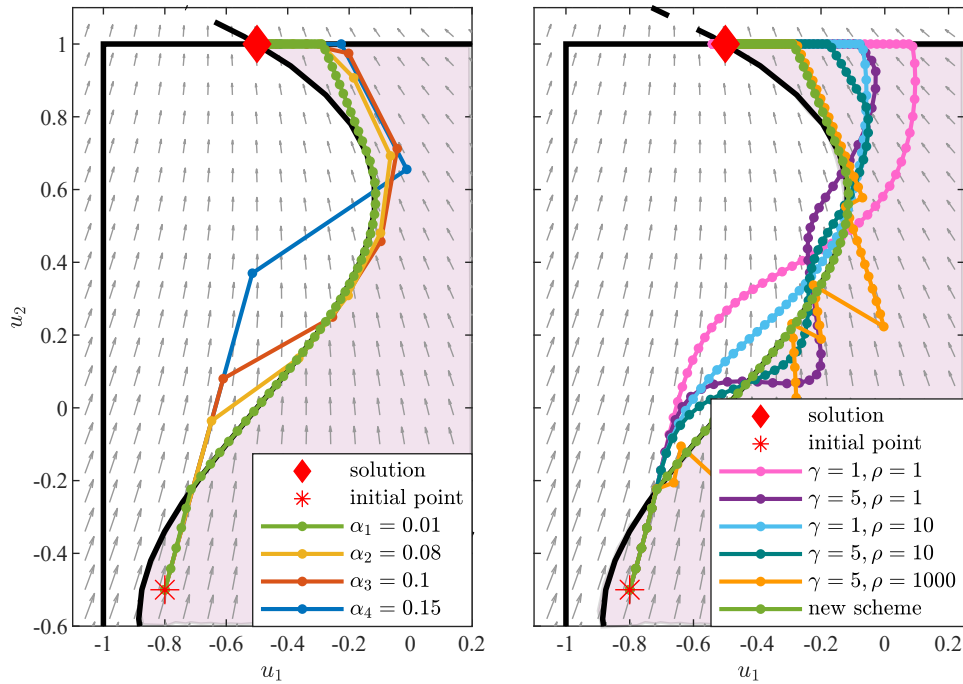


**Figure 18:** Comparison of the proposed iterative projected gradient flow (left), which converges to the always-feasible continuous time projected gradient flow for smaller step sizes, and augmented saddle point flows (right).

which are different for each bus). This reduces losses in the lines, and therefore minimizes the objective function. This voltage regulation is achieved via adequate reactive power compensation and tap changer position. Notice that in the approximate sensitivities that we used in the controller the effect of reactive power flows is neglected. Whether reactive power injections create or reduce losses depends on the concurrent reactive power demand at the load buses, and therefore this information cannot be used unless sensitivities are updated in real time. We refer to the discussion in D3.1 about how sensitivities can in fact be updated based on the current state of the grid.

Once wind generation sharply increases, overvoltage and line congestion is observed. Because of the latter, reactive power flows are reduced to zero (in order not to waste line capacity that is needed by the active power flows) and tap changers are used aggressively in order to maintain the voltage within acceptable values. Nonetheless, some active power curtailment is necessary. Notice that, in this second stage, voltages are significantly lower across the grid, at the cost of some additional losses. Notice also that wind generation curtailment is, cumulatively speaking, at acceptable levels. This is done by curtailing only a few specific generators which are critically placed with respect to the overloaded part of the grid. The majority of the generators are not curtailed.

This numerical study shows how the proposed principled approach, which can be tuned and designed by the grid operators based on their specifications (constraints) and priorities (cost function) is capable of producing a complex response and activate multiple concurrent services (reactive power compensation, tap changing, active power curtailment). Arguably, such a complex response in a such a short amount of time would not be attainable based on human expertise, primarily because the large number of controllable devices makes the problem high dimensional and interconnected. Moreover, individual heuristics for the single controllers (e.g., secondary voltage regulation schemes at the tap changers) are also insufficient for the task at hand, when clearly a coordinated strategy is required.

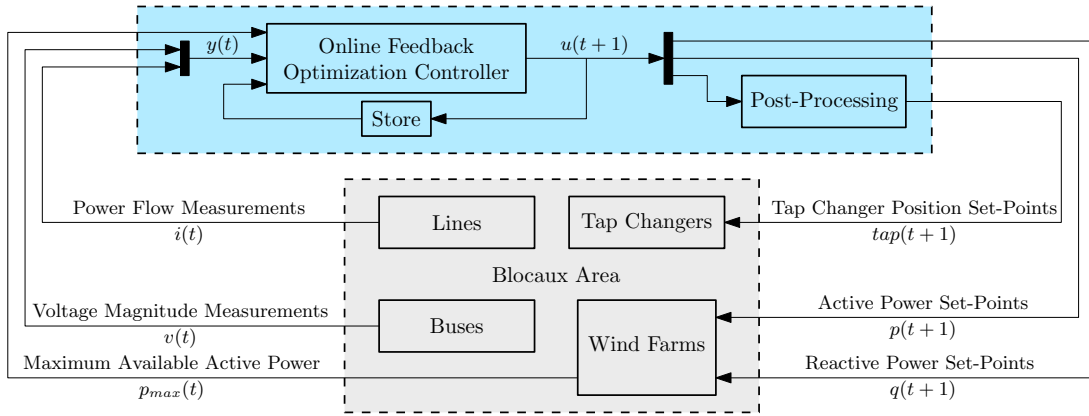


Figure 19: Control architecture employed for the UNICORN-7019 benchmark

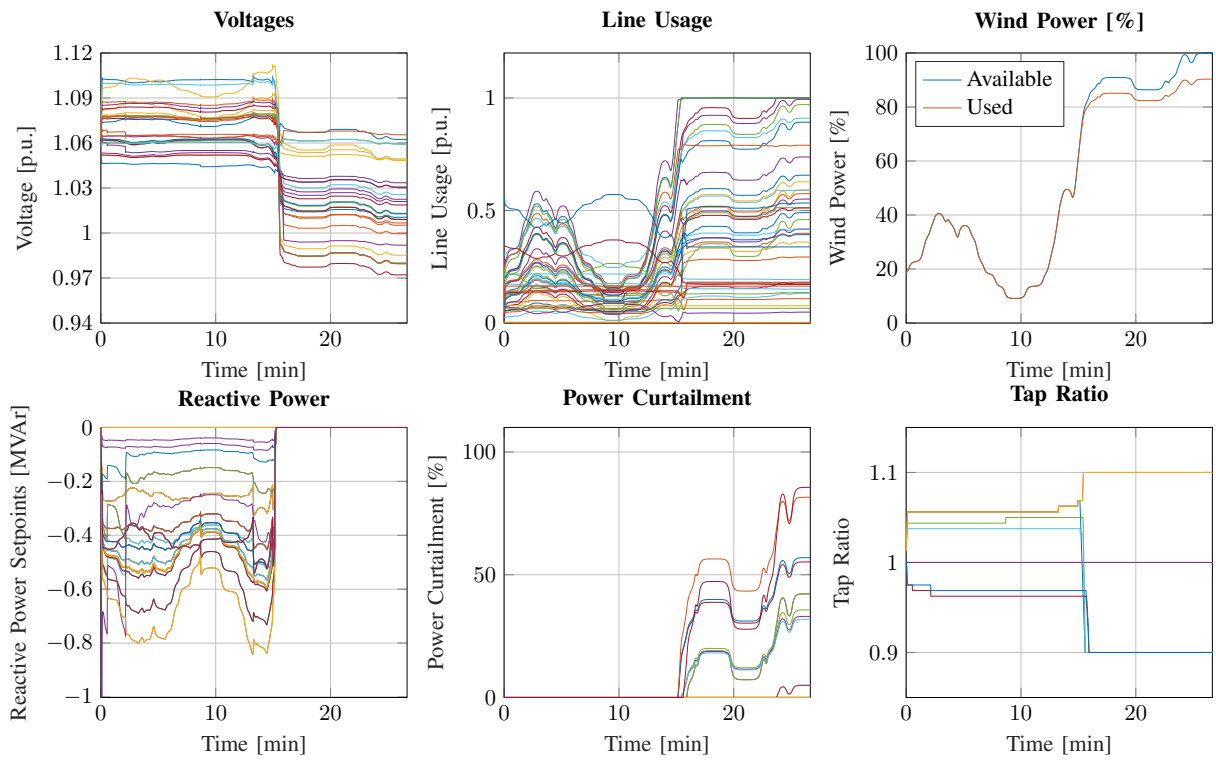


Figure 20: Simulation of the proposed real-time control strategy on the UNICORN-7019 subtransmission grid benchmark.



### 3.3 WP3 Engineering and experimental validation

In this last Work Package, the practicality of the proposed approach has been analyzed, to understand how it could be integrated in today grid's operation, and how the unified control scheme should be engineered.

#### D3.1 Control robustification

Throughout the simulations and the experiments in D2.2, we have assumed that measurements of the grid are available to the controller without delay. In a real setting, however, information on the state of the grid is often delayed, and the typically correspond to the output of some state estimator.

In [24], we studied the behavior of a feedback optimization scheme where, instead of assuming noise-free full state measurement, we connect a dynamic State Estimation using available measurements, and study its dynamic interaction with the optimization scheme. We certified stability of this interconnection and the convergence in expectation of the state estimate and the control inputs towards the true state values and optimal set-points respectively. The resulting architecture is represented in Figure 21.

We define by  $S$  the vector of active and reactive power injections in the grid, and by  $V$  the vector of voltage magnitudes and voltage phases (the state of the system).

We assumed that a linearized measurement equation is available and contains the measurements coming from all sources (e.g. conventional remote terminal units, smart meters, phasor measurement units, pseudomeasurements, etc.):

$$y = Hv + \omega_y, \quad (28)$$

where  $y$  is the vector of measurements,  $H$  is the matrix mapping the state to the measurements, and  $\omega_y$  is the measurement noise. We assume that this noise is Gaussian with known probability distribution  $\omega_y \sim \mathcal{N}(0, \Sigma_y)$ , and that using the pseudo-measurements, the matrix  $H$  has full-column rank, and thus the system is numerically observable.

We consider, for the stability analysis, the linearization of the power flow equations around the current operating point:

$$V = V_0 + B_c S_c + B_l S_l$$

where we have split the power injection into the controllable ones and the ones corresponding to time-varying loads. This corresponds to the following model for the state of the grid at subsequent times:

$$V_{(t)} = V_{(t-1)} + B_c(S_{c,(t)} - S_{c,(t-1)}) + \omega_{l,(t)}, \quad (29)$$

where  $\omega_{l,(t)} = B_l(S_{l,(t)} - S_{l,(t-1)})$  appears as a result of the time-varying load conditions  $S_{l,(t)}$ . Based on this simple dynamic model, we design a Kalman filter based state estimator, that at time  $(t)$  takes the measurements  $y_{(t)}$  as input and outputs the estimate  $\hat{V}_{(t)}$ :

$$\begin{aligned} \hat{V}_{(t)} &= (I_d - K_{(t)}H)(\hat{V}_{(t-1)} + B_c(S_{c,(t)} - S_{c,(t-1)})) + K_{(t)}y_{(t)} \\ P_{(t)} &= (I_d - K_{(t)}H)(P_{(t-1)} + \Sigma_l) \\ K_{(t)} &= (P_{(t-1)} + \Sigma_l)H^T (H(P_{(t-1)} + \Sigma_l)H^T + \Sigma_y)^{-1}, \end{aligned} \quad (30)$$

where  $I_d$  is the identity matrix,  $P_{(t)}$  denotes the covariance matrix of the voltage state estimate  $\hat{V}_{(t)}$ , and  $K_{(t)}$  is the Kalman gain matrix minimizing the resulting covariance  $P_{(t)}$ :  $K_{(t)} = \arg \min_K \text{trace}(P_{(t)})$ .

Therefore, instead of using the state  $V_{(t)}$  in the feedback optimization flow, we use  $\hat{V}_{(t)}$  from (30) as feedback to the projected gradient descent:

$$S_{c,(t+1)} = \Pi_{\mathcal{F}}[S_{c,(t)} - \epsilon(\nabla_{S_c} f(S_{c,(t)}) + B_c^T \nabla_V g(\hat{V}_{(t)}))], \quad (31)$$

where  $\Pi_{\mathcal{F}}$  denotes the projection on the set of feasible inputs (see D1.1).

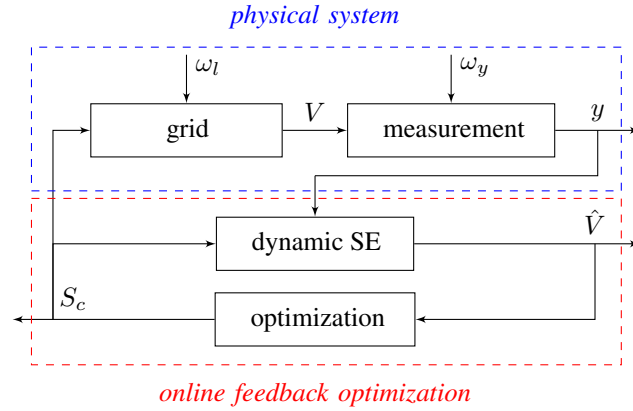


**Figure 21:** Feedback optimization architecture interconnected to a dynamic estimator of the grid state

The interconnection of these subsystems (30) and (31) with the stochastic dynamic system of the grid (29) and the measurement equation (28), results in the closed-loop system represented in Figure 21. However, even if the SE (30) converges in expectation to unbiased estimate with finite variance, and the online feedback optimization (31), converges asymptotically to the solution of the OPF, this does not guarantee that their interconnection will inherit these properties. Therefore, we verified the overall stability to ensure the desired behavior of this approach. The main stability result is reported as [24, Theorem 1] and states, under some technical assumptions, the following.

Let  $S_{c,(t)}^*$  be the optimal power injection that solves the given optimization problem at time  $t$ . Then both error terms  $\hat{V}_{(t)} - V_{(t)}$  and  $S_{c,(t)} - S_{c,(t)}^*$  are stochastic processes that quantify the estimation and the suboptimality, respectively. Then:

- the expected values of these errors converge towards 0
- their covariance is bounded.

This allows to conclude that the closed-loop stochastic dynamic system converges and is stable.

These results have been further developed. In [25] we demonstrated a similar statement (stability of the interconnection of feedback optimization, state estimation, and power flow solver) for the case on nonlinear power flow equations (see Figure 22). This extensions requires special care to deal with the nonlinearity, and one of the necessary steps was to carefully select a viable optimization flow and to robustify the interconnection with an additional “feedforward” term (which we proposed in [26]).

Nevertheless, the main message remains similar: real-time operation controllers based on feedback optimization are robust both to noisy measurements and to the dynamics introduced by state estimation routines.

In a similar spirit, in [23] we studied the interconnection of the proposed feedback control law with a Kalman-like estimator that has the task to identify the input-output sensitivity of the system based on past set-points and measurements (see Figure 23). As the sensitivities are the only piece of model information that is needed in order to execute the proposed feedback control law, this adaptive approach make the proposed scheme effectively model-free.

### D3.2 Proof-of-concept prototype

As described in D2.2, we delivered a proof-of-concept demonstration of feedback optimization for real-time power system operation by tackling the Volt/VAr regulation problem in benchmark UNICORN-4 [15]. A distributed (peer-to-peer) version of the controller has also been demonstrated [16].

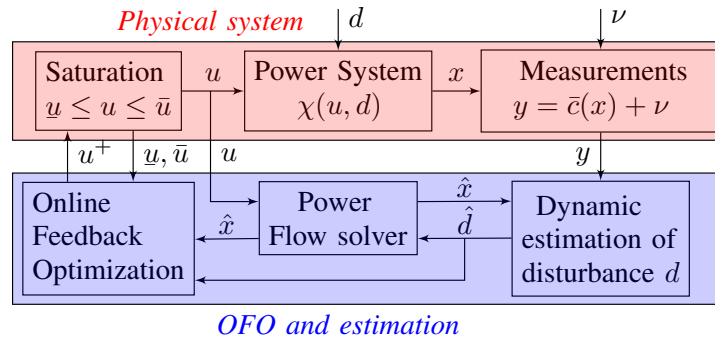


**Figure 22:** Block diagram representation of the interconnection of the feedback optimization routine, a state estimator, and its internal power flow solver, with the nonlinear physical grid. The stability of this closed loop is studied in [25].

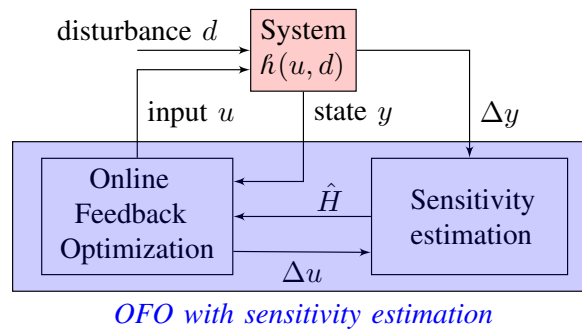


**Figure 23:** Block diagram representation of the interconnection of the feedback optimization routine and a sensitivity estimation routine, as proposed in [23].

In order to facilitate the repetition of these experiments, we provide a description of the power validation and testing procedure by adopting the nomenclature recommended in [27]. This nomenclature is adopted, for example, to propose experiments to be implemented on the ERIGRID network of laboratories (ERIGrid 2.0: European Research Infrastructure supporting Smart Grid and Smart Energy Systems Research, Technology Development, Validation and Roll Out, <https://erigrd2.eu>).

**Narrative** A power distribution feeder hosts a significant number of microgeneration sources, interconnected via electronic power converters, together with time-varying loads. The amount of microgeneration and load demand is such that, in some locations and at some times of the day, undervoltage and overvoltage phenomena occur (because of the non-negligible resistive nature of the lines and cables). The power converters can be controlled to inject or withdraw reactive power, up to some given limits (that can be function of the active power that is being injected/withdrawn at the same time). The test aims at showing that these power converters can be used as a network of reactive power compensators to regulate the voltage of the entire feeder, and therefore allow larger demands and generation with the same physical infrastructure. It also aims at showing that the full potential of these converters can be exploited only if they are coordinated via a communication channel, while purely local strategies fall short of this task. The inverter switching control architecture is out of scope of this specific test, and converters are assumed controllable via active and reactive power set points.

**Purpose of Investigation (PoI)** To characterize the tradeoff between communication (no communication » distributed communication » full centralization) and performance (the ability of regulating the voltages to some prescribed limits in the presence of time-varying demand and generation) for real-time control of distributed energy resources.



**System under Test (SuT)** The system under test is the distribution feeder, together with the power inverters that interconnect the microgenerators. The system is subject to the exogenous input of time-varying generation and demand, and is controlled by deciding the reactive power set points of the converters. Voltage magnitudes across the entire feeder are measured.

**Object under Investigation (Oul)** The networked feedback control law that regulates the reactive power set-points of the power converters in real time, based on the voltage measurements performed by same power converters.

**Domain under Investigation (Dul)** The electric power physical layer (only its steady state behavior), the control architecture, the communication layer.

**Function under Test (FuT)** Voltage measurement at the power converters, reactive power control at the power converters, peer-to-peer real-time communication between power converters, networked feedback control of reactive power injection for optimal voltage regulation.

**Function under Investigation (Ful)** Networked feedback control of reactive power injection for optimal voltage regulation.

#### **Test criteria**

- *Target criteria* – Effectiveness of voltage regulation, measured as the difference between the voltage profile achieved by the controlled system and the benchmark obtained by solving an offline Optimal Reactive Power Flow (ORPF) based on the collected exogenous data (generation and demands).
- *Variability attributes / Test factors* – The communication allowed between local controllers: no communication (purely local Volt/VAR control) vs full communication (centralized control). Different control strategies can be adopted for the centralized control scheme, based on which iterative optimization algorithm is implemented in closed loop with the system.
- *Quality attributes / Thresholds* – The fraction of time, in a time varying setting, when a centralized scheme is necessary (i.e., the fully local strategies are not sufficient) to track the benchmark solution of the ORPF.



## 4 Conclusions and next steps

The project demonstrated that feedback optimization can be used to design automated controllers for the real-time operation of the grid, and more specifically for reactive power compensation, active power curtailment, voltage regulation, tap changer control, losses minimization, line congestion control, and economic redispatch. While, as anticipated, these different tasks and functions can coexist in the same unified controller, we have identified some particularly promising setups, e.g., voltage regulation via reactive power compensation and tap changer control.

Among the problems that we imagine could be tackled most effectively by these tools are

- the coordinated control of microgenerators and energy resources in the distribution grid in order to minimize curtailment of active power (or, equivalently, in order to increase the hosting capacity of these grids)
- the coordinated control of tap changers and reactive power setpoints in the subtransmission grid in order to alleviate voltage regulation problems

Both these scenarios have been included in public benchmarks in order to stimulate further study in these directions.

A remarkable aspect of the proposed design tools is that they tap into the know-how and competence in the domain of nonlinear optimization. Closed-loop stability properties and convergence certificate have been provided by the analysis presented in this work, but they are not a concern of the practitioner that is called to apply these design methods to their specific instance of real-time operations. This is particularly valuable in a sector, power system operators, that has vast competence in the field of nonlinear optimization because of their planning and optimal power flow activities. The incorporation of the proposed real-time control method in the procedures of these operators is not expected to require the acquisition of new competences.

For the next steps, we envision three possible directions:

- **Engineering** – With all the steps from the development of the mathematical tools and certificates to the proof-of-concepts experimental demonstration, the project has done all the groundwork to allow an engineering phase for these ideas. Once some specific instances are identified, it is possible to adopt the design method proposed in this project and to complement them with the design and testing of appropriate communication architectures, data processing workflows, and secure implementations of the algorithms.
- **Emergency operations** – Some specific emergency operations in power systems, including restorative actions that are integral part of the N-1 security certificates, require the activation of a large number of energy resources in a short amount of time. When contingency become more complex and the number of available energy resources increases, the methods proposed in this project becomes a useful tool. In contrast to what has been studied in this project, emergency operation require special care when dealing with faster time-scales, unstable dynamics, and transient behaviors of the system.
- **Virtual reinforcement** – Many distribution grids and transmission grids are reaching their limit capacity when it comes to hosting renewable generation and, soon, a larger electric mobility demand. One possible solution is clearly to reinforce the grid via new “copper”, by installing new infrastructure, new devices, and new lines. We have shown in this project that, in some cases, a virtual reinforcement is possible: the grid capacity can be increased by deploying intelligence, sensing, and real-time control. With the correct economic incentives, virtual reinforcement of the power systems can be a very valuable tool (with up to billion of EUR in savings [28]).



## 5 International cooperation

A regular cooperation with the French transmission system operator RTE has continued in the second year. Regular remote monthly meetings have been organized. The following personnel at RTE have collaborated to the project:

- Patrick Panciatici, Scientific Advisor
- Jean Maeght, Research Engineer
- Marjorie Cosson, Research Engineer
- Manuel Ruiz, Research Engineer

RTE provided extensive expertise for the formulation of the real-time optimization scenario in power systems, together with real data from a congested portion of the subtransmission grid in France. They provided assistance in the numerical simulations, and helped to design specific numerical experiments to test the dynamic performance of the approach (based on their experience with integration of fluctuating wind generation).

## 6 Communication and dissemination

### 6.1 Public website and benchmarks

A public website has been created in order to make the output of the project accessible to researcher in academia and in industry, practitioners, and students.

<https://unicorn.control.ee.ethz.ch>

The website contains

- a summary of the main findings of the project,
- a link to the talks and tutorials that have been produced as part of the project (with slides and video recordings),
- a list of the peer-reviewed publications produced in the project, with links to open access preprints,
- downloadable numerical testbeds to replicate the findings of the project and to be used as benchmarks for alternative solutions to the problem of real-time control of power systems,
- downloadable Matlab/Simulink toolbox to simulate tap changer automatic behavior in MatPower simulations and to test feedback control strategies in closed loop with quasi-steady state power flow solvers.

### 6.2 Talks, tutorial, presentations

The results of the project have been regularly presented to the academic community, including both researchers in the fields and students in various institutions.

- "Virtual reinforcement of power grids: a feedback optimization approach"  
Workshop on Resilient Control of Infrastructure Networks  
Politecnico di Torino  
24 September 2019



- “Feedback optimization for real-time power system operation”  
Control seminar series at Peking University, China  
16 June 2020
- “Fully Distributed Peer-to-Peer Optimal Voltage Control with Minimal Model Requirements”  
XXI Power Systems Computation Conference (PSCC2020)  
29 June 2020
- “Experimental Validation of Feedback Optimization in Power Distribution Grids”  
XXI Power Systems Computation Conference (PSCC2020)  
29 June 2020
- “Closing the Loop: Dynamic State Estimation and Feedback Optimization of Power Grids”  
XXI Power Systems Computation Conference (PSCC2020)  
29 June 2020
- “Limit Behavior and the Role of Augmentation in Projected Saddle Flows for Convex Optimization”  
IFAC World congress 2020  
11 July 2020
- "Feedback Optimization for Real-Time Power System Operation"  
Workshop on Emerging Topics in Control of Power Systems  
KTH, Stockholm  
2 October 2020
- "Non-Convex Feedback Optimization with Input and Output Constraints"  
59th IEEE Conference on Decision and Control  
14 December 2020
- "A Unified Control Framework for Real-time Power System Operation"  
Workshop of the RTE Chair  
CentraleSupélec  
16 June 2021
- "A Feedback-Optimization Approach to Resilient Power System Operation"  
Workshop on Resilient Autonomous Energy Systems  
National Renewable Energy Laboratory (NREL), USA  
8 September 2021
- Plenary talk "Online Feedback Optimization with Applications to Power Systems"  
at Programme Gaspard Monge (PGMO DAYS) 2021  
30 November 2021
- Workshop "Towards a Systems Theory for Optimization Algorithms"  
at the 60th IEEE Conference on Decision and Control  
13 December 2021

A tutorial covering the necessary mathematical preliminaries, the problem formulation, and the project findings, has been organized for both academic and industrial researchers in the power system field.

- Tutorial "A Unified Control Framework for Real-Time Power System Operation"  
at IEEE SmartGridComm 2021  
25 October 2021

A similar tutorial has been proposed in order to reach also the control and optimization community:

- Tutorial "UNICORN – A Unified Control Framework for Real-Time Power System Operation"  
at IFAC Workshop on Control Applications of Optimization  
18-22 July 2022.



The results of the project, and in particular the mathematical methodology concerning the application of feedback optimization to real-time operation of power systems, have become substantial part of the 4-day graduate school “Control and Optimization of Autonomous Power Systems” organized as part of the International Graduate School on Control of the European Embedded Control Institute (EECI), see <http://www.eeci-igsc.eu>. The graduate school took place on 28 September–1 October 2020 in a virtual format, and was attended by 30 graduate students and researchers from academia and industry.

School website: <https://sites.google.com/view/eeci-igsc-m11>

The school will be offered again in summer 2022 in Stockholm.

## 7 Publications

On the topic of theory of feedback optimization:

- Verena Häberle, Adrian Hauswirth, Lukas Ortmann, Saverio Bolognani, Florian Dörfler  
"Non-Convex Feedback Optimization With Input and Output Constraints"  
IEEE Control Systems Letters, 2021, 5. doi: 10.1109/LCSYS.2020.3002152  
Open access preprint: <https://arxiv.org/abs/2004.0640>
- Adrian Hauswirth, Saverio Bolognani, Gabriela Hug, and Florian Dörfler  
"Timescale separation in autonomous optimization"  
IEEE Transactions on Automatic Control, 66(2), February 2021. doi: 10.1109/TAC.2020.2989274  
Open access preprint: <https://arxiv.org/abs/1905.06291>
- Adrian Hauswirth, Saverio Bolognani, Gabriela Hug, and Florian Dörfler  
"Optimization algorithms as robust feedback controllers"  
Under review. arXiv:2103.11329 [math.OC], 2021.  
Open access preprint: <https://arxiv.org/abs/2103.11329>

On the topic of real-time power system operation:

- Florian Dörfler, Saverio Bolognani, John W. Simpson-Porco, Sergio Grammatico  
"Distributed Control and Optimization for Autonomous Power Grids"  
European Control Conference (ECC), 2019. doi: 10.23919/ECC.2019.8795974  
Open access preprint: <https://www.research-collection.ethz.ch/handle/20.500.11850/363997>
- Miguel Picallo, Saverio Bolognani, Florian Dörfler  
"Closing the Loop: Dynamic State Estimation and Feedback Optimization of Power Grids"  
Electric Power Systems Research, 2020, 189, 106753. doi: 10.1016/j.epr.2020.106753  
Open access preprint: <https://arxiv.org/abs/1909.02753>
- Miguel Picallo, Dominic Liao-McPherson, Saverio Bolognani and Florian Dörfler  
"Cross-layer design for real-time grid operation: estimation, optimization and power flow"  
Electric Power Systems Research, to appear.  
Presented at the 22nd Power Systems Computation Conference (PSCC).  
Open access preprint: <https://arxiv.org/abs/2109.13842>
- Miguel Picallo, Lukas Ortmann, Saverio Bolognani and Florian Dörfler  
"Adaptive real-time grid operation via online feedback optimization with sensitivity estimation"  
Electric Power Systems Research, to appear.  
Presented at the 22nd Power Systems Computation Conference (PSCC).  
Open access preprint: <https://arxiv.org/abs/2110.00954>

On the experimental results:



- Lukas Ortmann, Adrian Hauswirth, Ivo Caduff, Florian Dörfler, Saverio Bolognani  
"Experimental Validation of Feedback Optimization in Power Distribution Grids"  
Electric Power Systems Research, 2020, 189, 106782. doi: 10.1016/j.epsr.2020.106782  
Presented at the 21st Power Systems Computation Conference (PSCC).  
Open access preprint: <https://arxiv.org/abs/1910.03384>
- Lukas Ortmann, Saverio Bolognani, Alexander Prostejovsky, Kai Heussen  
"Fully Distributed Peer-to-Peer Optimal Voltage Control with Minimal Model Requirements"  
Electric Power Systems Research, 2020, 189, 106717. doi: 10.1016/j.epsr.2020.106717  
Presented at the 21st Power Systems Computation Conference (PSCC).  
Open access preprint: <https://arxiv.org/abs/1910.03392>

## References

- [1] D. K. Molzahn, F. Dörfler, H. Sandberg, S. H. Low, S. Chakrabarti, R. Baldick, and J. Lavaei, "A survey of distributed optimization and control algorithms for electric power systems," *IEEE Trans. Smart Grid*, vol. 8, no. 6, pp. 2941–2962, Nov. 2017.
- [2] L. Gan and S. H. Low, "An online gradient algorithm for optimal power flow on radial networks," *IEEE J. Sel. Areas Commun.*, vol. 34, no. 3, pp. 625–638, Mar. 2016.
- [3] E. Dall'Anese and A. Simonetto, "Optimal power flow pursuit," *IEEE Trans. Smart Grid*, vol. 9, no. 2, pp. 942–952, Mar. 2018.
- [4] Y. Tang, K. Dvijotham, and S. Low, "Real-time optimal power flow," *IEEE Trans. Smart Grid*, vol. 8, no. 6, pp. 2963–2973, Nov. 2017.
- [5] A. Bernstein and E. Dall'Anese, "Real-time feedback-based optimization of distribution grids: A unified approach," *IEEE Trans. Control Netw. Syst.*, vol. 6, no. 3, pp. 1197–1209, Sep. 2019.
- [6] S. Bolognani and F. Dörfler, "Fast power system analysis via implicit linearization of the power flow manifold," in *53rd Annual Allerton Conference on Communication, Control, and Computing (Allerton)*, 2015.
- [7] A. Hauswirth, S. Bolognani, G. Hug, and F. Dörfler, "Projected gradient descent on Riemannian manifolds with applications to online power system optimization," in *54th Annual Allerton Conference on Communication, Control, and Computing (Allerton)*, 2016.
- [8] —, "Optimization algorithms as robust feedback controllers," *arXiv:2103.11329 [math.OC]*, 2021. [Online]. Available: <https://arxiv.org/abs/2103.11329>
- [9] H. K. Khalil, *Nonlinear Systems*, 3rd ed. Upper Saddle River, NJ: Prentice Hall, 2002.
- [10] A. Hauswirth, S. Bolognani, G. Hug, and F. Dörfler, "Timescale separation in autonomous optimization," *IEEE Transactions on Automatic Control*, vol. 66, no. 2, pp. 611–624, Feb. 2021. [Online]. Available: <https://arxiv.org/abs/1905.06291>
- [11] "Commission regulation (EU) 2016/631 of 14 april 2016 establishing a network code on requirements for grid connection of generators," *OJ*, vol. L112, pp. 1–68, 2016.
- [12] "VDE-AR-N 4105: generators connected to the LV distribution network - technical requirements for the connection to and parallel operation with low-voltage distribution networks," 2018.
- [13] IEEE 1547-2018, "Standard for interconnection and interoperability of distributed energy resources with associated electric power systems interfaces."



- [14] S. Bolognani, R. Carli, G. Cavraro, and S. Zampieri, "On the need for communication for voltage regulation of power distribution grids," *IEEE Trans. Control Netw. Syst.*, vol. 6, no. 3, pp. 1111–1123, Sep. 2019. [Online]. Available: [http://people.ee.ethz.ch/~bsaverio/papers/Bolognani\\_TCNS\\_2019.pdf](http://people.ee.ethz.ch/~bsaverio/papers/Bolognani_TCNS_2019.pdf)
- [15] L. Ortmann, A. Hauswirth, I. Caduff, F. Dörfler, and S. Bolognani, "Experimental validation of feedback optimization in power distribution grids," *Electric Power Systems Research*, vol. 189, p. 106782, Dec. 2020, presented at the 21st Power Systems Computation Conference (PSCC). [Online]. Available: <https://arxiv.org/abs/1910.03384>
- [16] L. Ortmann, A. Prostejovsky, K. Heussen, and S. Bolognani, "Fully distributed peer-to-peer optimal voltage control with minimal model requirements," *Electric Power Systems Research*, vol. 189, p. 106717, Dec. 2020, presented at the 21st Power Systems Computation Conference (PSCC). [Online]. Available: <https://arxiv.org/abs/1910.03392>
- [17] S. Bolognani and S. Zampieri, "On the existence and linear approximation of the power flow solution in power distribution networks," *IEEE Trans. Power Syst.*, vol. 31, no. 1, 2016.
- [18] W. H. Kersting, "Radial distribution test feeders," in *IEEE Power Engineering Society Winter Meeting*, vol. 2, Jan. 2001, pp. 908–912.
- [19] R. Pedersen, C. Sloth, G. B. Andresen, and R. Wisniewski, "DiSC: A simulation framework for distribution system voltage control," in *European Control Conference (ECC)*, 2015.
- [20] S. Bolognani, "networked-volt-var - A comparison of Volt/VAR feedback control laws: fully decentralized vs networked strategies," GitHub, 2018. [Online]. Available: <https://github.com/saverioB/networked-volt-var>
- [21] S. Bolognani, R. Carli, G. Cavraro, and S. Zampieri, "On the need for communication for voltage regulation of power distribution grids [source code]," CodeOcean, May 2019. [Online]. Available: <https://doi.org/10.24433/CO.8982151.v1>
- [22] V. Häberle, A. Hauswirth, L. Ortmann, S. Bolognani, and F. Dörfler, "Non-convex feedback optimization with input and output constraints," *IEEE Control Systems Letters*, vol. 5, no. 1, Jan. 2021. [Online]. Available: <https://arxiv.org/abs/2004.06407>
- [23] M. Picallo, L. Ortmann, S. Bolognani, and F. Dörfler, "Adaptive real-time grid operation via online feedback optimization with sensitivity estimation," *arXiv:2110.00954 [eess.SY]*, 2021. [Online]. Available: <https://arxiv.org/abs/2110.00954>
- [24] M. Picallo, S. Bolognani, and F. Dörfler, "Closing the loop: Dynamic state estimation and feedback optimization of power grids," *Electric Power Systems Research*, vol. 189, p. 106753, Dec. 2020, presented at the 21st Power Systems Computation Conference (PSCC). [Online]. Available: <https://arxiv.org/abs/1909.02753>
- [25] M. Picallo, D. Liao-McPherson, S. Bolognani, and F. Dörfler, "Cross-layer design for real-time grid operation: Estimation, optimization and power flow," *Electric Power Systems Research*, to appear, presented at the 22nd Power Systems Computation Conference (PSCC). [Online]. Available: <https://arxiv.org/abs/2109.13842>
- [26] M. Picallo, S. Bolognani, and F. Dörfler, "Predictive-sensitivity: Beyond singular perturbation for control design on multiple time scales," *arXiv:2101.04367 [math.OC]*, 2021. [Online]. Available: <https://arxiv.org/abs/2101.04367>
- [27] M. Blank, S. Lehnhoff, K. Heussen, D. E. M. Bondy, C. Moyo, and T. Strasser, "Towards a foundation for holistic power system validation and testing," in *21st IEEE Intl. Conf. on Emerging Technologies and Factory Automation (ETFA)*, 2016.
- [28] RTE, "Schéma décennal de développement du réseau," Tech. Rep., 2019. [Online]. Available: <https://www.rte-france.com/analyses-tendances-et-prospectives/le-schema-decennal-de-developpement-du-reseau>